A review on non-destructive evaluation of construction materials and structures using magnetic sensors

Eslamlou, Armin Dadras; Ghaderiaram, Aliakbar; Schlangen, Erik; Fotouhi, Mohammad

DOI
10.1016/j.conbuildmat.2023.132460

Publication date
2023

Document Version
Final published version

Published in
Construction and Building Materials

Construction and Building Materials 397 (2023) 132460

Contents lists available at ScienceDirect

Construction and Building Materials

journal homepage: www.elsevier.com/locate/conbuildmat

Review

A review on non-destructive evaluation of construction materials and structures using magnetic sensors

Armin Dadras Eslamlou [a,b], Aliakbar Ghaderiaram [c], Erik Schlangen [c], Mohammad Fotouhi [c,*]

[a] School of Civil Engineering and Transportation, South China University of Technology, Guangzhou 510640, China
[b] China-Singapore International Joint Research Institute, Guangzhou 510700, China
[c] MICROLAB, Faculty of Civil Engineering and Geosciences, Delft University of Technology, Delft, the Netherlands

ARTICLE INFO

Keywords:
Magnetic Sensors
Construction Materials
Eddy Current
Magnetic Flux Leakage
Hall Effect
Magnetoresistive Sensors
Magnetoelastic
Magneto-mechanical sensors
Electromagnetic Sensors
Magnetostrictive Sensors

ABSTRACT

The growing demand towards life cycle sustainability has created a tremendous interest in non-destructive evaluation (NDE) to minimize manufacturing defects and waste, and to improve maintenance and extend service life. Applications of Magnetic Sensors (MSs) in NDE of civil Construction Materials to detect damage and deficiencies have become of great interest in recent years. This is due to their low cost, non-contact data collection, and high sensitivity under the influence of external stimuli such as strain, temperature and humidity. There have been several advancements in MSs over the years for strain evaluation, corrosion monitoring, etc. based on the magnetic property changes. However, these MSs are at their nascent stages of development, and thus, there are several challenges that exist. This paper summarizes the recent advancements in MSs and their applications in civil engineering. Principle functions of different types of MSs are discussed, and their comparative characteristics are presented. The research challenges are highlighted and the main applications and advantages of different MSs are critically reviewed.

1. Introduction

Civil construction materials are the building blocks for structures and infrastructures such as buildings, facilities, wind turbines, tunnels, and bridges with a significant place within the economy and play an important role in facilitating the standard of living for the world population. These materials and structures are experiencing premature damage and can reach their end of life earlier than expected [1]. Replacing such structures is time-consuming, labor-intensive and costly, therefore, a variety of non-destructive evaluation (NDE) techniques have been used to evaluate the safety and structural integrity of these structures in order to reduce the financial losses, as well as avoid catastrophic failure for health and safety issues [2]. NDE can reduce maintenance costs while improving reliability and safety, creating more sustainable infrastructures by providing effective maintenance and better resource allocation. Furthermore, it results in increasing service life and reducing the rate of consumption of resources and waste generation.

Different NDE techniques have been used in civil applications, some examples are visual inspection, optical fiber sensing, resistance strain gauges, piezoelectric transducers, vibration and modal analysis, and electric and electromagnetic (EM) techniques [3]. Despite all the advantages, NDE usage is limited in civil structures as it is costly, labor-intensive, and difficult to implement. The sensing equipment can be susceptible to failure under harsh environmental conditions, and installation of the systems with cabling and dedicated positions requires extensive time and labor efforts. Innovative NDE methods are currently being investigated to overcome the technical challenges of conventional methods. Extensive research and progress have been made especially during the last decade on the use of magnetic sensors (MSs) for NDE [4]. MSs offer several advantages such as elevated sensitivity, reduced size and the ability to perform as a self-powered sensor [5]. An MS reacts to the presence or the interruption of a magnetic field by generating a proportional output. Fig. 1 shows a summary of the main MSs used in different applications, reflecting a rich and diverse measurement range and accuracy.

This review paper provides up-to-date information on progress made on different types of MSs, their working principle and their applications, with some insights on their performance and reliability. Fig. 2 presents the distribution of reviewed papers on MSs over time. A surge of interest is being shown in the application of MSs to structural health monitoring of civil materials and structures since 2018. In this review, we conducted

* Corresponding author.
E-mail address: M.Fotouhi-1@tudelft.nl (M. Fotouhi).

https://doi.org/10.1016/j.conbuildmat.2023.132460
Received 14 December 2022; Received in revised form 4 May 2023; Accepted 8 July 2023
Available online 12 July 2023

an extensive literature search on Google Scholar, using a combination of relevant keywords, such as "magnetic," "sensor," "non-destructive," "damage," "defect," "crack," "health," "structure," "material," "construction," and "civil." We screened the search results and eliminated irrelevant articles outside the scope of this review. We found that Magnetic Flux Leakage (MFL), Eddy current, Magnetoelastic, EM, Hall effect, magnetoresistive (MR), magnetomachnaical, microwire, magnetostrictive, and smart rock sensors were the most frequently studied, in descending order. Therefore, this paper will focus on the most studied MS technologies for NDE in civil engineering applications. For each of them, a brief description of the principle of operation, example applications and recent developments are provided.

2. Magnetic sensors

2.1. Hall effect sensors

According to the Hall effect [8], when a current is applied to a thin strip of a conductor in the presence of a magnetic field perpendicular to the direction of the current, the charge carriers are deflected by Lorentz force. Therefore, an electric potential difference is created between two sides of the strip, as shown in Fig. 2. The voltage difference (Hall voltage) is proportional to the strength of the magnetic field. The Hall effect sensor detects the presence and magnitude of a magnetic field by measuring the voltage variation when subjected to a fixed (non-changing) magnetic field.

Zhu et al. [9] developed mobile Hall effect sensors to evaluate the structural integrity of steel structures, and it was concluded that this method is capable of detecting the damage and its location. Two types of damage were simulated by an extra mass block and loosened bolts, and transmissibility function analysis was used for signal processing.

Fernandes et al. [10] used Hall effect sensors by integration of MFL-main magnetic flux (MMF) signals, for the detection of corrosion and fracture in prestressed strands of prestressed concrete structures. They concluded that the MFL signal can detect the presence of corrosion and strand breaks, while the MMF signal can estimate the loss of steel due to corrosion. This system was demonstrated to be a promising tool for box-beam inspection of bridges. Zhang et al. [11] developed a method for detecting and measuring the amount of corrosion in concrete reinforcements, using Hall effect measurement principles as shown in Fig. 3. The developed magnetic system can be embedded in concrete and has a good capacity for quantitative analysis of corrosion rate.

Alonso et al. [12] created a permanent magnetic field using a simple magnetic structure, as shown in Fig. 4 and measured the magnetic field with a Hall effect sensor. According to the measurements, when the steel was in the path of magnetic fluxes, the intensity of the magnetic field density increased by about 25%, providing a simple, economic, and non-invasive MS for the measurement of the changes in internal stress in pieces of steel.

Table 1 presents a summary of the above-reviewed papers.

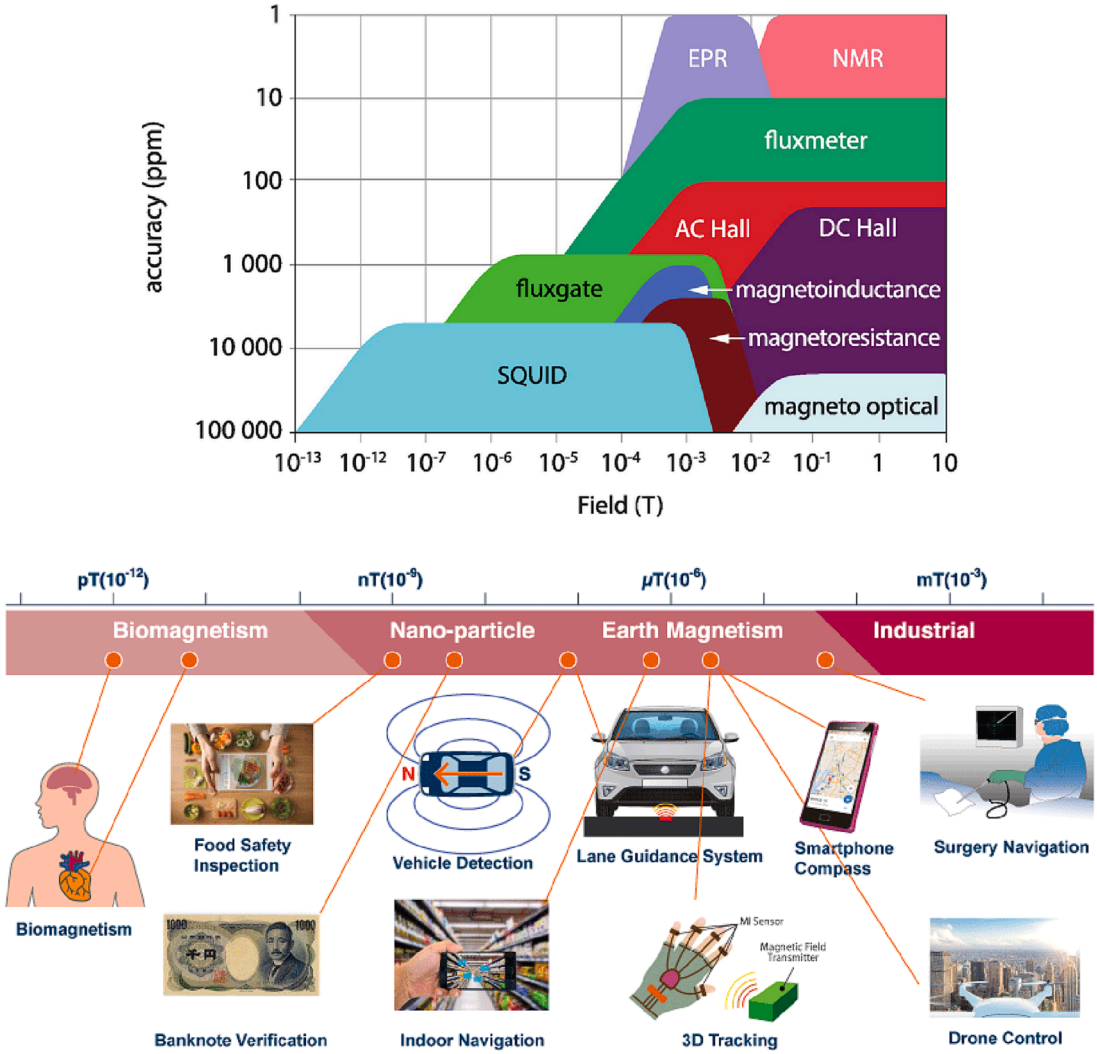

Fig. 1. Classification of important field sensing techniques, by measurement range and accuracy [6], the detectable magnetic field strength of the MSs [7].

2.2. Magnetoresistive sensors

In 1857, William Thomson discovered that the electrical resistance of a ferromagnetic material changes through an external magnetic field, called the magnetoresistive effect [13]. It took more than 100 years before the first MR sensor was developed by Hunt in 1971. Generally, there are three categories of MR sensors, namely anisotropic magnetoresistance (AMR), giant magnetoresistance (GMR) and tunneling magnetoresistance (TMR) sensors. The basic structure of each type of MR element is illustrated in Fig. 5.

The resistance in AMR sensors depends on the angle between the current and the magnetization direction, where the resistance is in the smallest level at a 90-degree angle and it is in the highest level when the current is parallel [14]. GMRs feature 10 to 15% further magnetoresistance compared to AMR devices, and it is the reason for coining the prefix 'giant'. They involve very thin layers of ferromagnetic materials such as iron, and non-magnetic conductive materials such as copper. GMR devices have equal responses to positive or negative fields, but their sensitivity to perpendicular fields is small [14]. Additionally, the GMRs are able to operate at fields above the operating range of AMRs [15]. In TMR sensors, the electrical resistance becomes the smallest when the magnetization directions of the pin layer and free layer (as shown in Fig. 5) are parallel, causing a large current to flow into the barrier layer [16]. But the resistance becomes extremely large when the magnetization directions are antiparallel.

Nicholson, et al. [17] developed an MR sensor-based system to scan a defected surface in steel and other ferromagnetic materials. Wincheski, et al. [18] developed a self-nulling GMR sensors for the inspection of deep flaws, they highlighted favorable performance of the sensors under different environmental conditions, and their lower power consumption, high sensitivity, small size and sufficient depth of penetration. Chady [15] used GMR sensors for quantitative stress evaluation and associated stress damage in steel samples. He defined three straightforward indexes based on the voltage signal from the sensors. The measuring time for scanning an area of 41 cm^2 was about 10 min which can be reduced by using an array of sensors. Additionally, the method requires some preliminary treatments such as magnetization and demagnetization of samples before testing because the results are dependent on the magnetic history of the samples. Lo, et al. [19] developed a magnetic imaging system capable of measuring hysteresis and Barkhausen effect signals using MR sensors. It can measure subsurface notches and stress distribution in ferrous materials. Popovics, et al. [20] applied GMR sensors for corrosion sensing in concrete structures. They showed that corroding steel bars exhibit higher levels of magnetic noise as well as higher field gradients. Procházka and Vaněk [21] studied blade damage identification through a tip-timing technique which is based on the time difference of blade passages. To extract the time differences, they used MR sensors that detect the blades made with

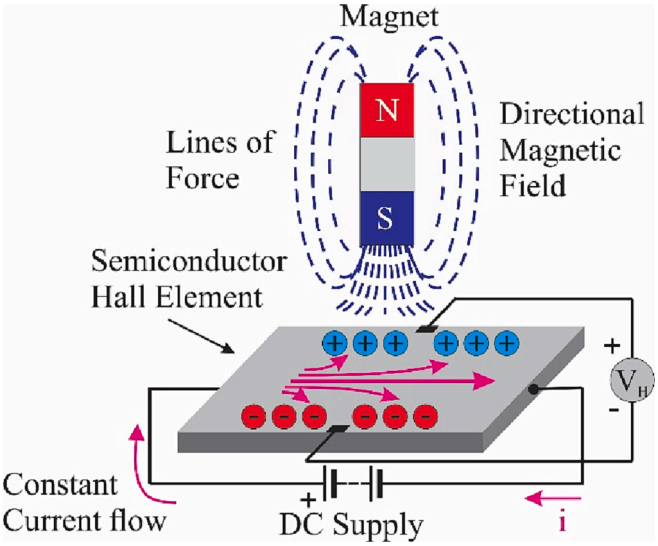

Fig. 3. Working principle of the Hall effect sensor.

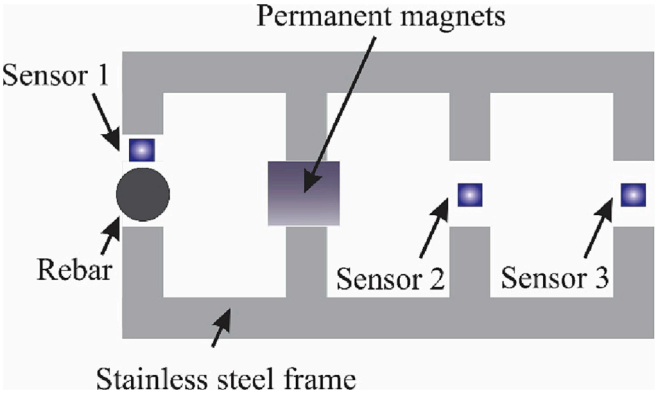

Fig. 4. Schematic diagram of the magnetic-based corrosion evaluation design.

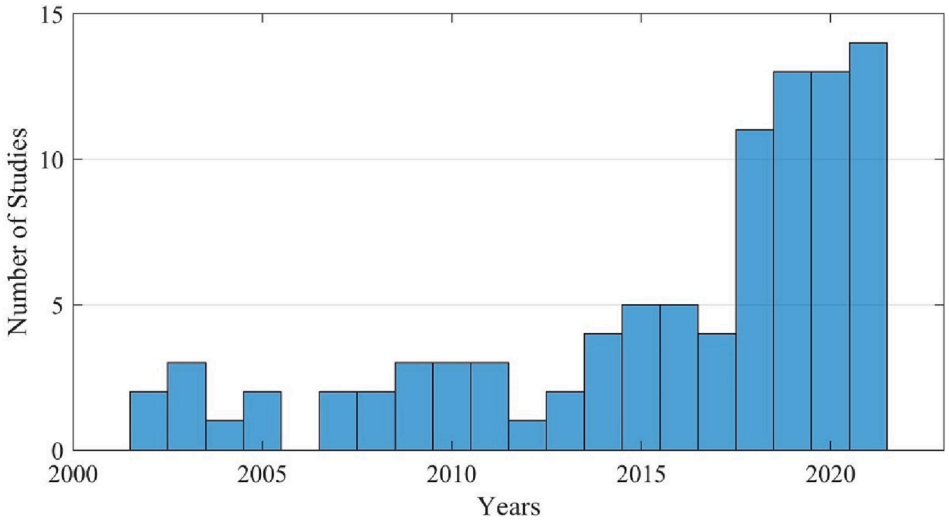

Fig. 2. The growing trend in the number of published research studies on MSs.

Table 1
Types of structures and damages examined by Hall effect sensors.

Reference	Year	Damage type, application and main features
Zhu, et al. [9]	2010	Extra mass block and lossened bolts detections in steel strucutres - Flexible system architectures with adaptive and high spatial resolutions - Wide transmission range - Real-time - Wireless communication
Fernandes, et al. [10]	2014	Corrosion and fracture detection in pre-stressed steels in reinforced concrete such as box-beam of bridges - Lag between the MMF and MFL signals - Low power usage - Lightweight
Zhang, et al. [11]	2017	Corrosion in reinforced concrete - High precision - Assess corrosion rate
García Alonso, et al. [12]	2020	Stress in steel structures - Not limited to measuring the surface local strain

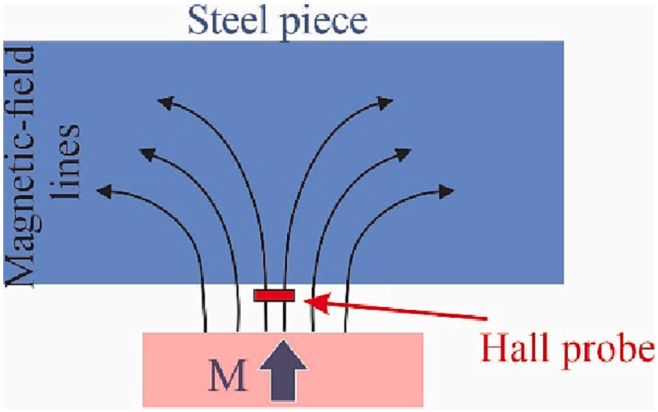

Fig. 5. Scheme of the device with the magnetic fields.

ferromagnetic material and studied the amplitudes and time differences of generated impulse signals. Yang, et al. [22] utilized two unidirectional coils oriented in orthogonal directions that outperform the traditional unidirectional coils that cannot detect cracks parallel to the direction of linear currents. A GMR sensor was applied to measure the flux density of the induced field. Tsukada, et al. [23] developed a magnetic measuring system for detecting steel plate thickness and inner corrosions. The system includes an induction coil for applying an AC magnetic field to the plate and an AMR sensor for detecting the normal magnetic component. It was shown that the phase spectrum extracted from the magnetic spectrum is a reliable feature for thickness detection, and moreover, the differential magnetic vector shortens the measurement time and reduces the influence of liftoff.

Table 2. provides a detailed overview of the applications of MR sensors in the literature.

2.3. Eddy current sensors

Eddy currents are induced by changing magnetic fields and currents in closed loops perpendicular to the magnetic field plane (Fig. 6). They circulate in conductor-like rotating vortices, and can occur when a conductor moves in a magnetic field, or when the magnetic field around a fixed conductor is variable. The size of the eddy current is proportional to the size of the magnetic field, the area of the ring, and the rate of change of the magnetic flux, and is inversely proportional to the conductive resistance. Like any current passing through a conductor, an eddy current creates its own magnetic field. The Lenz law states that the

Table 2
Types of structures and damages examined by MR sensors.

Reference	Year	Damage type, application and main features
Nicholson, et al. [17]	1996	Surface defects in ferromagnetic structures - Limited by the dimensions of the MR sensor - Useful for low data density magnetic media
Wincheski, et al. [18]	2002	Deep fatigue cracks in fastener holes - Small size - High sensitivity - Ease of use - Low power requirements - Double SNR over previous GMR-based methods
Chady [15]	2002	Stress degradation in ferromagnetic structutes - Small size of the sensors - Straightforward measurement - High sensitivity to material degradation - Tolerance to external noises and lift-off changes - Very low cost of sensors - Quantitative evaluation of applied stresses
Lo, et al. [19]	2003	Surface defects in ferromagnetic structures - High sensitivity- Wide bandwidth (megahertz and above) - Small size - Capable of measuring both magnetic hysteresis and Barkhausen effect signals
Popovics, et al. [20]	2007	Corrosion in Reinforced concrete - Wide sensing range - Favorable environmental performance- Low power consumption (powered by 5-V battery)
Procházka and Vaněk [21]	2011	Elongation and untwisting in turbine blades - Sensing frequencies up to 10 MHz - Suitable for tip speeds up to 700 m/sec - Detects 1 μm deflections - Unable distinguish between blade position drift and a position change of blades due to a crack development - Contactless - High sensitivity
Yang, et al. [22]	2015	Cracks in layered structures - Linear sensitivity over a broad range of frequencies - Detecting crack orientations - Low cost - Low power supply requirements - Small size
Tsukada, et al. [23]	2016	Inner corrosions in steel structures - High-speed imaging - High SNR

direction of the magnetic-induced current, like an eddy current, will be such that the generated magnetic field opposes the change in the magnetic field that creates it. In general, if the conductor to be tested is perfectly uniform and without defects, the magnetic field resulting from the eddy currents must also be uniform. Otherwise, if there is a defect or crack in the conductor, it changes the magnetic field caused by the eddy current. This method can be applied for evaluating a wide range of near-the-surface defects and cracks in civil structures with magnetic properties.

Zilberstein, et al. [24] designed a meandering winding eddy current sensor with a linear array. After analyzing the output signals of the meandering winding magnetometer sensor, they were able to quantitatively evaluate the fatigue life percentage and even early detection of cracks in a steel specimen. Ricken, et al. [25] applied eddy current coils to detect stress in prestressed strand wires in reinforced concrete structures. Sodano [26] applied a coil to detect damage in an aluminum plate using the principle of eddy currents. With the occurrence of damage or corrosion on the conductive surface, the amount of mutual induction in the coil changes, and as a result, by measuring the impedance of the coil at different excitation frequencies, the location of damage can be detected. Park, et al. [27] developed a pulsed eddy current sensor to measure the wall thickness of steel pipes. An advantage of this application is that there is no need to remove the pipe cover, and

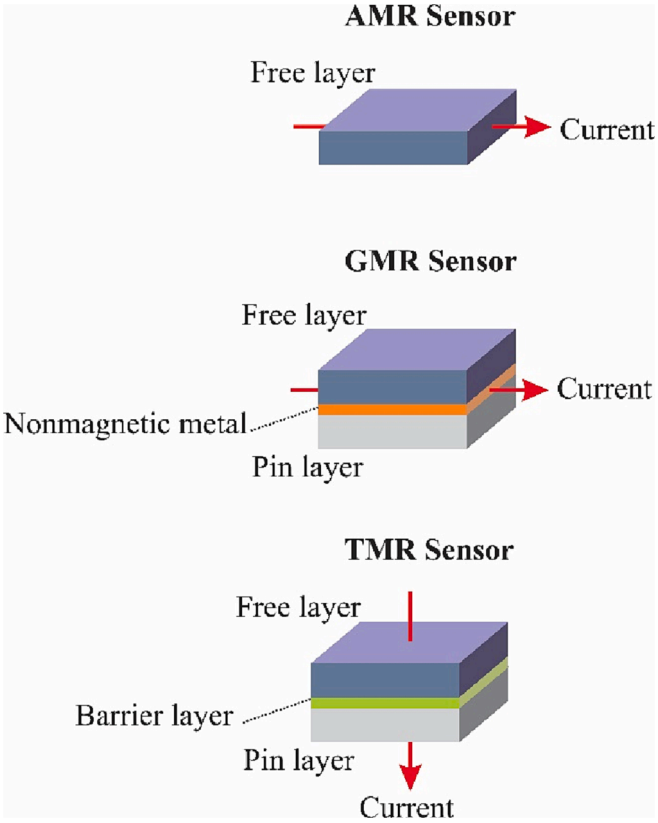

Fig. 6. Schematic diagram of AMR, GMR and TMR sensors.

the thickness of the pipe walls can be measured from a distance of 6 mm. Cao, et al. [28] were able to design a system that detects broken strands and defects in wire ropes, using the effect of eddy current. They used two coils placed in a circle around the wire rope (as shown in Fig. 7). In the excitation coil (U_i), alternating current is applied that causes eddy currents in wire ropes. Then, the magnetic field resulting from these eddy currents induces a voltage in the detecting coil (U_o). Using quantitative analysis based on radial basis function neural networks, they investigated defects in the rope by the signal from the eddy current sensor.

Wincheski and Simpson [29] integrated MR sensors with eddy current probes. They designed a new eddy current probe incorporating a dual induction source which can detect flaws in various depths. Torres, et al. [30] presented a multi-sensor scanner system based on eddy current and MR sensors to monitor suspension bridge cables. By using the proposed system, the corrosion through thick barriers was detected and the suitability of the resolution and the sensitivity of the MR sensors were indicated. Xiu, et al. [31] used a coil and a test specimen as the solenoid core, similar to elastomagnetic sensors. In the measurements, the sensor impedance was used as a measure of the amount of tension. They showed that the impedance of the eddy current sensor has an inverse relationship with the amount of applied tension. In their circuit model, which is seen in Fig. 8., R0 and L0 are the values of the resistance and inductance of the coil without specimen, C_0 is the effect of coaxial cable capacitors and the capacitive effects of adjacent coil turns. L_1 and R_1 are also the effects of eddy currents from the specimen under test.

Chen, et al. [32] developed a flexible eddy current sensor to monitor cracks in welded structures. First, they performed experiments using the classical eddy current sensors, and also simulated this sensor using CAMSOL software and examined the effects of cracks. Then, by making changes in the magnetic field excitation coil they were able to achieve higher sensitivity in detecting cracks. Tsukada, et al. [33] and Hayashi, et al. [34] designed a crack detection sensor in ferromagnetic materials using the eddy current method and, instead of employing a detector coil, applied TMR probes achieving linear and 2-D scan of surface cracks. The advantage of this method compared to classical eddy current sensors is that the magnetic field of the excitation coil does not affect the crack detection signal. Sun, et al. [35] designed and fabricated a flexible eddy current sensor in a thin film substrate. The thin film sensor was wrapped around the bolt and placed at the junction (as shown in Fig. 9). It can monitor the bolt junction hole in two dimensions and detect the presence of cracks as well as their growth.

Sun, et al. [36] performed similar research to [19], but with the difference that in this study, the eddy current sensor arrays were arranged vertically and placed around the bolt to monitor cracks and their growth in the bolt. Xie, et al. [37] presented an idea to detect defects in the body of long metal pipes by eddy current detection. A magnetic field excitation coil was placed around a tube and a detector coil was placed inside the tube (Fig. 10). According to the numerical results and experimental observations, the output voltage of the sensor had acceptable changes in the face of defects in the tube body.

Mukherjee, et al. [38] developed eddy current sensors capable of detecting corrosion in reinforced concrete rebars. In this system, as can be seen in Fig. 11, a very sensitive AMR sensor was used to detect magnetic fields generated by eddy currents. They used the amount of phase shift to determine the amount of corrosion.

Liu, et al. [39] attempted to construct an eddy current sensor in a flexible substrate to measure bearing failure in a Carbon-Fiber-Reinforced Polymers (CFRP) bolted joint. The structure of this system is the same as [19] and [20], meaning that a flexible sensor array consisting of induction and excitation coils was installed around the coil and measured the structural integrity changes. Guilizzoni, et al. [40]

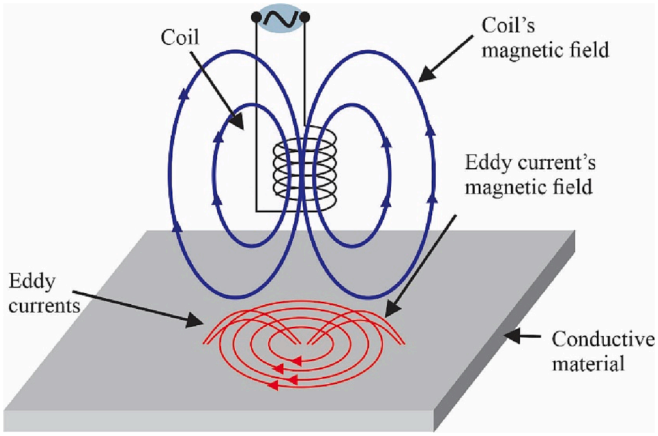

Fig. 7. Schematic of how eddy currents work.

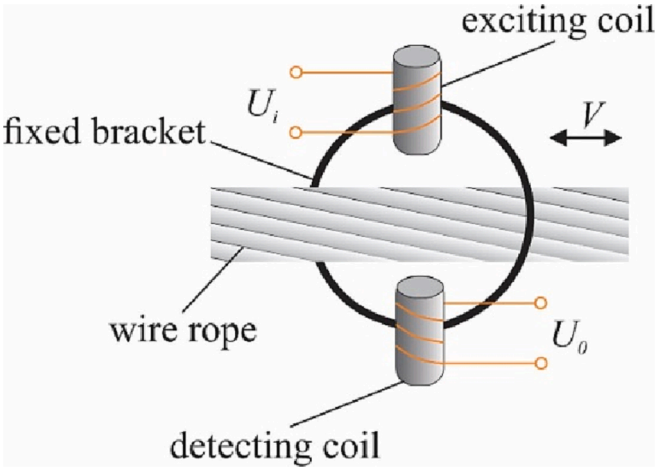

Fig. 8. Schematic of the eddy current detection setup.

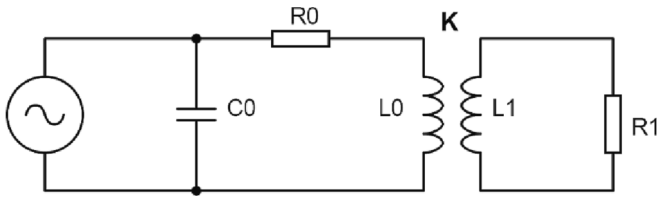

Fig. 9. Inductor–resistor–capacitor model of eddy current sensor.

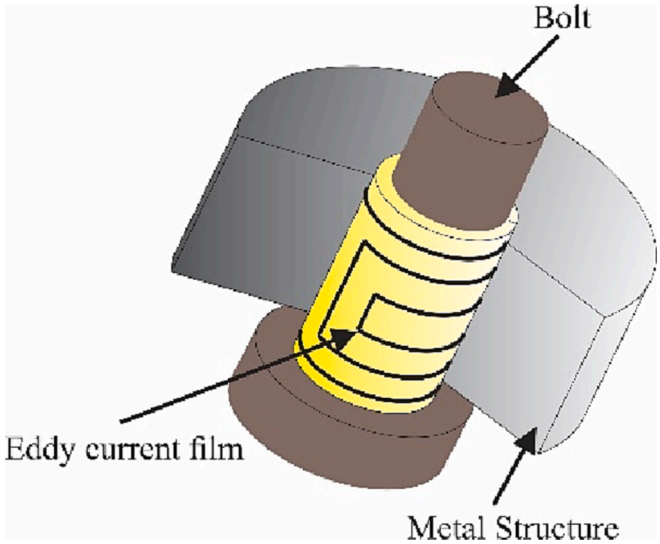

Fig. 10. Eddy current sensor wrapped around the bolt and placed at the junction.

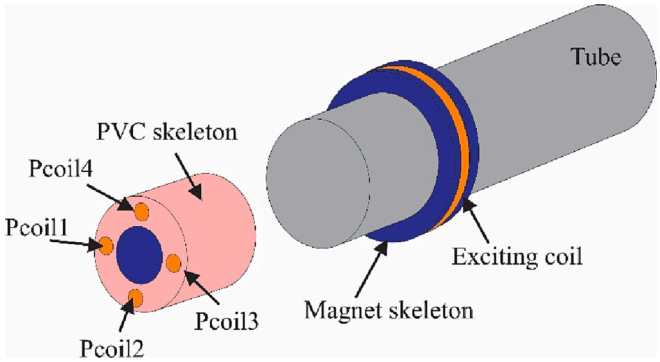

Fig. 11. Structure of magnetic force transmission eddy current array probe.

presented a method based on low-frequency eddy-current induction, which is able to detect wall losses in multilayered steel structures including an insulating gap. Since corrosion has the same effect as changes in thickness, it can be used for corrosion detection.

Table 3 provides an overview of the applications of eddy current sensors in the literature. As reviewed above, the usual method of generating a variable magnetic field is to use an AC coil. Researchers have used various techniques to receive and detect the magnetic field of the eddy current. In many cases, coils have been used for detection, and in some cases to increase the accuracy of MSs, such as Hall effect or TMR sensors. Due to the fact that this method requires a time-varying magnetic field, the excitation current frequency of the exciter coil is important. According to research, high frequencies for surface monitoring and low frequencies for depth monitoring provide better results [41].

Table 3
Types of structures and damages examined by eddy current method.

Reference	Year	Damage type, application and main features
Zilberstein, et al. [24]	2003	Fatigue life evaluation and early crack detection of XX - High-resolution imaging - Highly reliable and repeatable - Capability of detecting short cracks
H. A. Sodano [26]	2007	Damage and corrosion in an aluminum panel - Highly reliable and repeatable - Low cost manufacturing
Park, et al. [27]	2009	Thickness of steel pipes - High spatial resolution - Less power consumption - Peforming better than pickup coils for detecting sub-surface defects
Cao, et al. [28]	2012	Broken strand and defects in wire ropes - High sensitivity - High speed - Non-contact
Wincheski and Simpson [29]	2011	Flaw detection in aluminum structures - Operation from low frequency deep flaw detection to high frequency high resolution near surface material characterization.
Torres, et al. [30]	2011	Corrosion in steel cables - Investigating penetration depth change by the frequency range of 50 Hz to 1KHz
C. Xiu et al. [31]	2017	Tension in steel - Single-coil structure - Small size - Low cost
Chen, et al. [32]	2018	Crack in welded structutures - The sensitivity of the sensor is at least 19 times that of the original sensor.
Tsukada, et al. [33]	2018	Crack in steel plates - High signal-to-noise ratio (SNR)
Hayashi, et al. [34]	2019	Crack in steel structures - New design for reducing the magnetic noise.
Sun, et al. [35]	2019	Crack in bolted joints - FEM simulation is utilized to study the interaction between eddy current signals and the damage - flexible film designing sensor
Sun, et al. [36]	2020	Crack in bolted joints - Micron-width crack detection - High magnetic permeability
Xie, et al. [37]	2020	Defect in steel pipes - Fast detection - Low cost - High accuracy - Applicability to both ferromagnetic and non-ferromagnetic materials
Mukherjee, et al. [38]	2020	Rebar corrosion in reinforced concrete structures - Phase sensitivity - Quantifying volume loss
Liu, et al. [39]	2021	Bearing failure in CFRP joints - Easy operation - High sensitivity - Low cost

2.4. *Electromagnetic sensors*

EM waves have the ability to propagate in different environments and are affected by different materials (as shown in Fig. 12), therefore they can be used to measure the properties of different materials. When magnetic field waves propagate in the environment, they are affected by ferromagnetic materials such as iron and steel, and their intensity and direction change. Using this feature, we can monitor both inside and outside of the ferromagnetic materials in civil structures.

Chen, et al. [42] used an innovative coaxial cable as an external electrical conductor. The cable was installed along a concrete beam, the return pulses were measured, and the location and severity of failure were determined from the ratio of the returning pulse amplitude and time. Rumiche et al. [43,44] investigated the structural properties of carbon steel alloys using the EM method. By combining an EM sensor

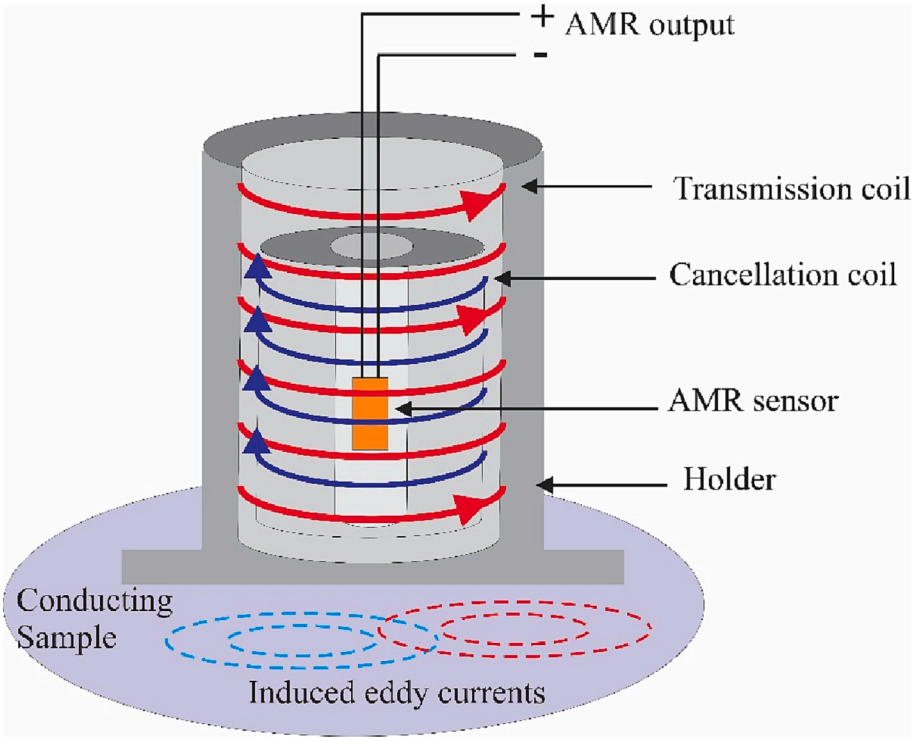

Fig. 12. Phase sensitive detection of corrosion system using eddy currents.

consisting of two coils (a primary coil to excite the magnetic field and a secondary solenoid to sense the magnetic field) and a Hall effect sensor they were able to find a relationship between the size of the grains and the percentage of alloys with the output signal as well as changes in the cross section.

Herdovics and Cegla [45] monitored the health of steel pipes, using the EM method and eddy current measurement technique. They installed an array of EM elements along the circumference of a pipe and used them to monitor the forces acting on the pipe. Arango, et al. [46] designed an antenna that can act as a passive sensor using EM waves and detect the presence of cracks in structures. The general principle of the system was based on a cavity tuned to a specific frequency (2.4 GHz) through which the connected antenna can communicate wirelessly with the reference system. Li, et al. [47] investigated the corrosion of concrete reinforcement, combining EM and acoustic emission methods, in which they detected the location of cracks and the degree of rust of a rebar inside the concrete. In addition, in ref. Li, et al. [48], they were able to process and analyze the signals received from the EM sensor through digital image correlation.

Fu, et al. [49] used the EM method and a Hall effect sensor to measure and test corrosion in reinforced concrete reinforcements. They used an EM coil with a specific core, which is illustrated in Fig. 13. In this method, by placing the sensor in the corners of columns and concrete beams, and applying EM field, the degree of corrosion of rebars inside the concrete can be measured from outside by Hall effect sensors.

Diogenes, et al. [50] used a yoke and two coils at its ends (as shown in Fig. 14) to detect and measure the diameter of carbon rods in reinforced concrete. Different waveforms were applied to stimulate magnetic fields and the effect and efficiency of each were measured.

Frankowski, et al. [51] utilized a different EM method to detect the amount of corrosion and cross-sectional loss of rebars in reinforced concretes. Fig. 15 shows a schematic of how this system works. Its working principle is that by applying a variable magnetic field into the reinforced concrete, magnetic waves propagate along the rebars and are converted into mechanical displacement by a permanent magnet. The displacement of the magnet was measured with an electronic

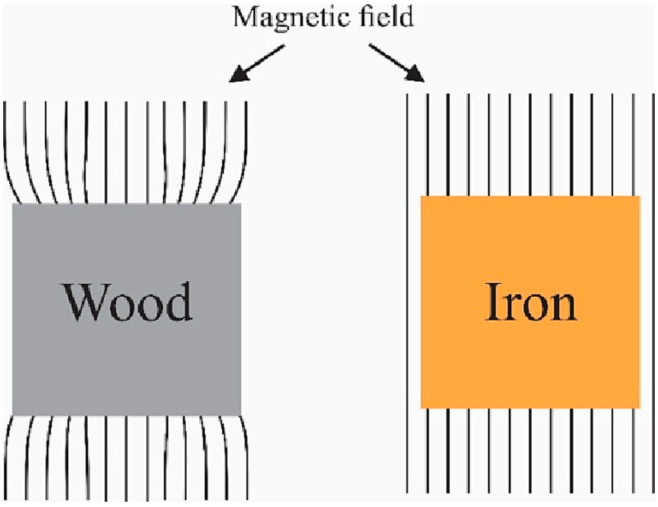

Fig. 13. Schematic example of the affectability of the magnetic field in the face of materials.

accelerometer, and the received information was analyzed to determine the amount of decay and debonding. The greater the amount of rebar decay, the greater the cross-sectional loss and the less the connection with concrete.

The details of the reviewed references are presented in Table 4. It was reported that the EM method is very extensive and can identify desired parameters based on material behaviors and mechanical properties. In most cases, variable and adjustable magnetic fields, conventional coils with different shapes and configurations or yokes [50] were used to have a combination of magnetic fields. The coil or Hall effect integrated circuit sensors [43,44,47–49] were applied to receive the magnetic response, in a passive antenna [46] or for receiving vibration response [51].

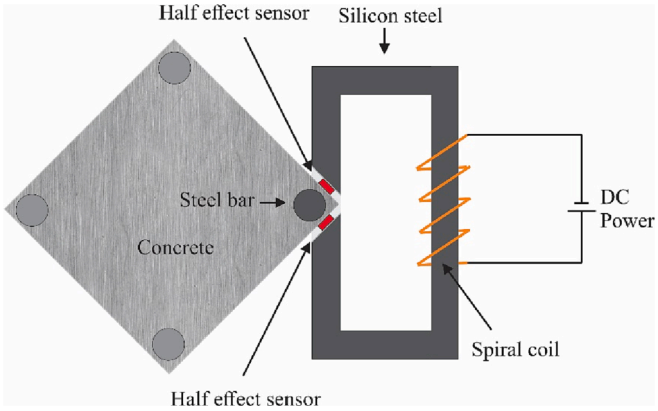

Fig. 14. Schematic illustration of the external EM sensor.

2.5. Magnetoelastic sensors

The operating principles of this type of this NDE system are based on the conversion of the elastic force on cables or ferromagnetic materials into an electrical signal. In magnetoelastic sensors, the element is monitored at the core of the magnetic coil and acts as a magnetic flux conductor media. In most cases, there is a secondary coil to induce the EM signal. In another version of the sensor, there is only one self-inducting inductor, and the cable acts as a magnetic core. By applying tensile force, the magnetic properties of the cable (ferromagnet core) change, causing a change in its magnetic permeability and, consequently, a change in the output signal. By analyzing the characteristics of the output signal, the amount of tension and stress applied to the cable or concrete girder can be extracted. Fig. 16 shows a schematic of the magnetoelastic sensor mechanism and how the primary and secondary coils are placed around the cable.

Sumitro, et al. [52] used two coaxial magnetic coils in such a way that the wire or cable is placed as the core of the coils. By applying a tensile force to the cable, its magnetic property changes and as a result, the amount of EM induction of the primary coil to the secondary coil changes. The effect of the temperature on the amount of permeability has a direct relationship with the tensile force applied to the cable. Ausanio, et al. [53] made an MS with a ribbon core of an amorphous alloy. In this sensor, two coils were located around a tube, and the alloy ribbon in the middle was suspended by applying a compressive or tensile force to the ribbon core, the length of the ribbon changes, which consequently changes the resonant frequency of the sensor. Kim, et al. [54] put an MS inside a pre-stressed concrete girder (as seen in Fig. 17). In these experiments, the magnetic permeability was measured, which decreases by increasing the amount of tensile force.

Ren, et al. [55] used voltage-to-current ratio instead of induced voltage to reduce the measurement error caused by the voltage drop. An image of the investigated sensor is shown in Fig. 18. In an experiment, using ME sensors, they measured the tension of the radial and circular cables of a stadium by the voltage-induced method and the voltage-to-current ratio method. Using the ratio method measurement improves the relative efficiency of the sensor by 11%.

Zhang, et al. [56] studied the compensation of error due to temperature changes in the classical magnetoelastic sensor with primary and secondary coils. In order to compensate for the changes of temperature, in the range of $-10^{\circ}C$ to $60^{\circ}C$, they used artificial neural networks (ANNs). The prediction of the amount of force after the temperature compensation was very close to the actual value, with a maximum error of 0.9%. Zhang, et al. [57] investigated the measurement of tensile strength of steel cables using a magnetoelastic method, with the difference that instead of using excitation and secondary coils, they used the self-induction method. Kim and Park [58] installed ME sensors in the middle of cables for estimating the stress in cables. They used the values of magnetic density, magnetic field strength ratio (magnetic permeability) as well as the real tensile force recorded by the

Table 4
Types of structures and damages examined by EM method.

Reference	Year	Damage type, application and main features
Chen, et al. [42]	2004	Cracks in reinforced concrete beams - Can be over 15–80 times more than commercial flexural tests of RC beams
Rumiche et al. [43,44]	2008	Structural and morphological properties of steel - A linear correlation between B_s and the mass loss was found in all cases.
Herdovics and Cegla [45]	2016	Mass addition to pipes - The random noise level in the ultrasonic signal is less than 240 dB
Arango, et al. [46]	2019	Crack in aluminum sheets - Crack growing identification
Li et al. [47,48]	2020	Corrosion in reinforced concrete structures - The apparatus was miniaturized in order to improve the signal-to noise ratio - Using differences in permeability to detect the reinforced corrosion - Coupling of application of EM sensors and digital image correlation technique
Fu, et al. [49]	2020	Corrosion in reinforced concrete structures - The change of magnetic flux density has a good accuracy in estimating the mass loss of steel - Steel bar, as a ferromagnetic material, possesses a 100 times higher permeability than corrosion products
Diogenes, et al. [50]	2021	Rebar diameter monitoring in concrete structures - Two waveforms were used in order to improve the resolution of the hysteresis curve
Frankowski, et al. [51]	2021	Corrosion in reinforced concrete structures - Examining the bond between rebars and concrete with higher sensitivity - Fully non-contact - Achieving high sensitivity and repeatability

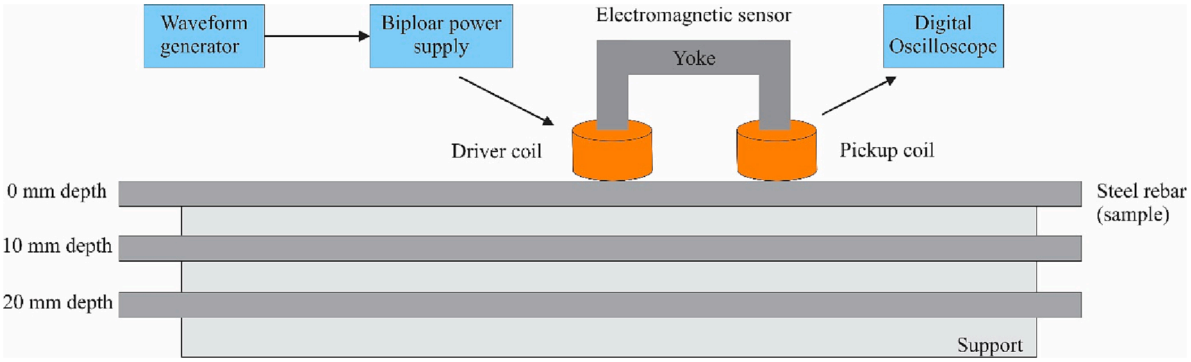

Fig. 15. Diagram of the experimental device. Dimensions are in millimeters.

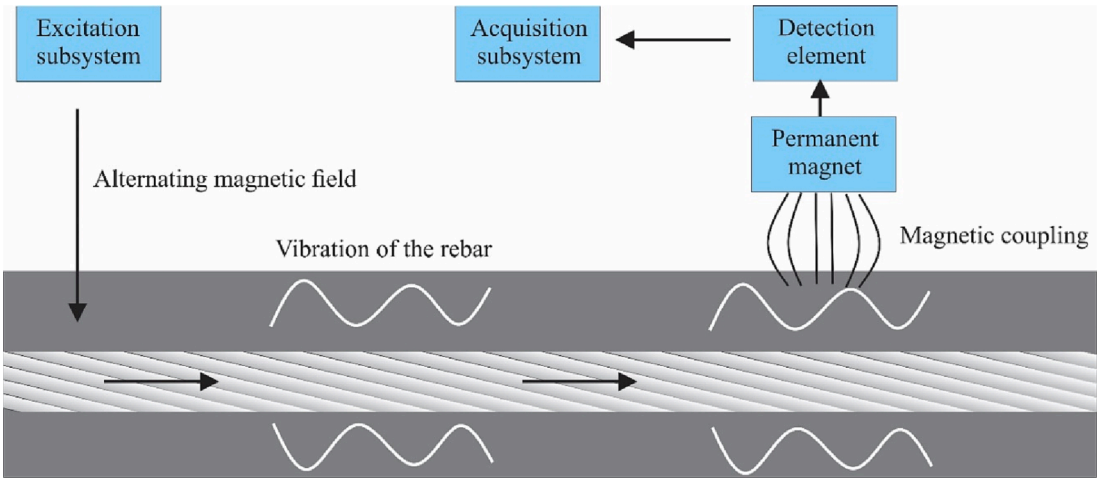

Fig. 16. Working principle of Magnetic force induced vibration evaluation (M5) method.

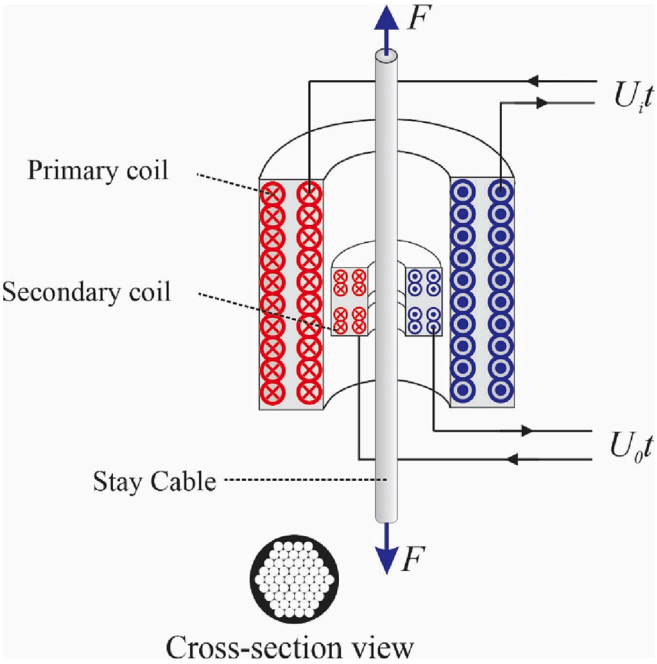

Fig. 17. Schematic of a magnetoelastic sensor.

Fig. 18. Embedded EM sensor and its sheath on carbon steel tendon as core (taken from [54]).

load cells to train and estimate force values using different machine learning algorithms. Kim, et al. [59] conducted research on the applicability of embedded magnetoelastic sensors to measure the tensile strength of prestressed concrete girders. According to the measurements, the area of the hysteresis curve was inversely related to the elastic force. Feng, et al. [60] used a magnetoelastic sensor with a pulsed power source to measure the stress of bridge cables, as seen in Fig. 19. It was observed that, in the time domain, the parameters measured in the sensor were significantly dependent on the temperature.

Zhang, et al. [61] did research with the aim of investigating the history of elastic force in monitoring the force of cables. It was concluded that if the fluctuations in tension are less than 30% of the design tension, the secant line of the unloading stage can be used to calculate the approximate tension with an error of less than 10%, otherwise, the relative monitoring error will reach 20%.

Table 5 provides a detailed overview of the applications of magnetoelastic sensors in the literature. The use of magnetoelastic sensors consisting of primary and secondary coils as well as self-inducting inductors has advantages such as high sensitivity to stress and magnetic permeability and the ability to be buried in concrete. In most cases, the amount of stress applied to cables or girders is converted to a graph (B-H), and features such as the hysteresis area of a curve or the loading–unloading phase curve are used to find the relationship between changes in the force applied to cables or concrete girders and changes in permeability is inverse.

The sensitivity of the sensor to the temperature and EM waves of the environment cannot be ignored. To the noise and errors caused by the EM waves in the environment, a metal shield is usually deployed to cover the perimeter of the sensor. The problem of temperature dependence is very important because it can cause a shift in the output voltage diagram or cause an error in the extracted amount of permeability. In this regard, several solutions have been proposed: using pulse excitation

Fig. 19. EM sensor (taken from [55]).

Table 5
Types of structures and measurements examined by magnetoelastic sensors.

Reference	Year	Damage type, application and main features
Sumitro, et al. [52]	2003	Tensile force of steel cable - Less than 10% error - Resistant to water and mechanical injury - Over 50 years service life
Ausanio, et al. [53]	2005	Tensile force of metal structures - About 200 times higher sensitivity compared with the vibrating wire strain gauge - About 4 times higher sensitivity than resistive strain gauge
Kim, et al. [54]	2017	Tensile force of PSC tendons - Measuring the magnetic responses of unrevealed PS tendon located inside the concrete
Ren, et al. [55]	2018	Tensile force of steel cable - Less than 8.3% relative error - Large measurement range - Long life - Not requiring physical contact - Linear relationship between the measured parameter and tension - Real-time
Zhang, et al. [56]	2018	Tensile force of steel cable - The maximum relative error of measurement is within ±0.9% - The root mean square error is less than 0.4
Zhang, et al. [57]	2019	Tensile force of steel cable - High sensitivity - Real-time - Easy installation
Kim and Park [58]	2020	Tensile force of steel cable- The maximum error rate of radial basis function network (RBFN) was 7.5% while that of feedforward neural network (FNN) was 9.8%
Kim, et al. [59]	2019	Tensile force of PSC tendons - Short measurement time - Small equipment size
Feng, et al. [60]	2019	Tensile force of steel cable - Less sensitive to temperature. - Fast - Unaffected by manual operations
Zhang, et al. [61]	2021	Tensile force of steel cable - Considering high-stress levels. - Establishing a relationship between the inductance increments and stress

signal instead of AC signal to reduce power loss and heat output, numerical methods to compensate for the effect of temperature on the output signal and predicting the amount of net pressure using curve fitting, neural network and machine learning, as well as frequency signal analysis in the frequency domain. If the temperature dependence becomes eliminated or minimized, this method can be an attractive option for measuring the tensile force or stress in structural elements.

2.6. Magnetic flux leakage

A permanent magnet or an electromagnet in the form of a yoke can generate a nearly uniform magnetic field. By placing a ferromagnetic object in the field, it can be magnetized and work as a magnet. As a result of the crack, an air gap forms between the two sides. Since the air gap cannot transmit as much magnetic field per unit volume as the ferromagnetic object, the magnetic field spreads out. The larger the flaw, the more MFL. Putting a sensor, such as a Hall sensor, near the damaged area, MFL can be detected, and the damage can be identified. This mechanism is illustrated in Fig. 20. Having measured the MFL signal, statistical or signal processing techniques might be applied to improve the signal resolution and detection accuracy.

Park *et al.* [62] proposed an inspection system to localize damage in steel cables, as shown in Fig. 21. They designed and manufactured an 8-channel MFL sensor equipped with one Hall sensor installed in each channel. It was observed that the sensing intensity is sensitive to the

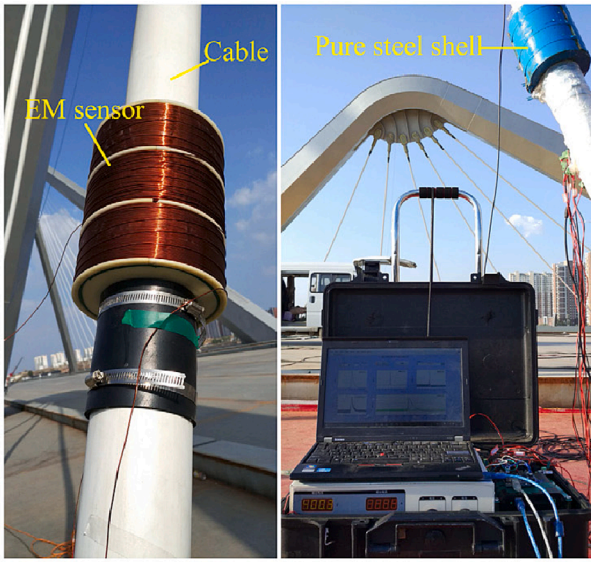

Fig. 20. The field test pictures of magnetoelastic sensor (taken from [60]).

distance, thus a threshold, based on generalized extreme value (GEV) distributions, was determined to detect damage locations with a confidence level of 99.99%.

Sun *et al.* [63] provided an MFL-based open magnetized method for online health monitoring of ferrous ropes through changes in signals. They developed rigid and free tracking ring-shaped variants of the device, as illustrated in Fig. 21, and compared them with the traditional yoke magnetization method. They showed that the approach produces less friction, which leads to higher service life in comparison with conventional sensors. Further, it is robust against shaking noise and indicates a higher sensitivity to damage. Sakai *et al.* [64] developed a ferrite yoke equipped with an MR sensor to detect backside-defects such as acid and galvanic corrosion of steel plates. By measuring the magnetic field, the system was able to detect changes correlated with the position and thickness reduction of the plate. Park *et al.* [65] applied a yoke-type electromagnet to magnetize the cable and utilized an openable search coil to measure the total magnetic flux over the area of the coil. This apparatus is shown in Fig. 21. Kim *et al.* [66] applied an extremely low-frequency alternating current (ELF-AC) to a primary coil at the EM yoke to magnetize cables, and a search coil sensor to measure the flux. As shown in Fig. 21, the apparatus was similar to that of Ref. [65]. They provided a relationship between the slope and cross-sectional loss. Kim and Park [67] fabricated a sensor module including two pairs of yokes, made with high-strength Nd-Fe-B permanent magnets, plates of carbon steel as magnetizers, and Hall sensors as signal measurement components. A schematic of this equipment is illustrated in Fig. 21. After measuring and processing the signals, the GEV distribution was used to localize damage with a 99.99% confidence level. Moreover, to quantify damage, they proposed three new indexes, namely the peak value of envelope (E_p), the width of the envelope (E_w) and the area of the envelope (E_A), and tested their sensitivity to width, depth, and length of damage. Compared with traditional peak-to-peak value ($P\text{-}P_v$) and peak-to-peak width ($P\text{-}P_w$) indexes, the proposed width and area of envelope indexes featured more reliability in quantifying the mentioned damage severities. These indexes are depicted in Fig. 22.

Kim and Park [68] continued their previous study (Ref. [67]) in several aspects. First, to increase the sensitivity of the device and cover wider angles of circumference, they increased the number of channels to 8, as shown in Fig. 21. Second, another index called Full Width at Half Maximum (FWHM) was proposed in addition to previously introduced indexes. It was shown that $P\text{-}P_v$, E_v, E_w, and E_A have positive correlations with damage depth. FWHM and P-Pw indicate increasing patterns as the

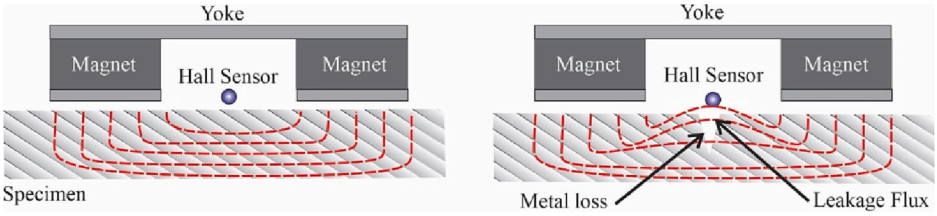

Fig. 21. A schematic of the MFL method.

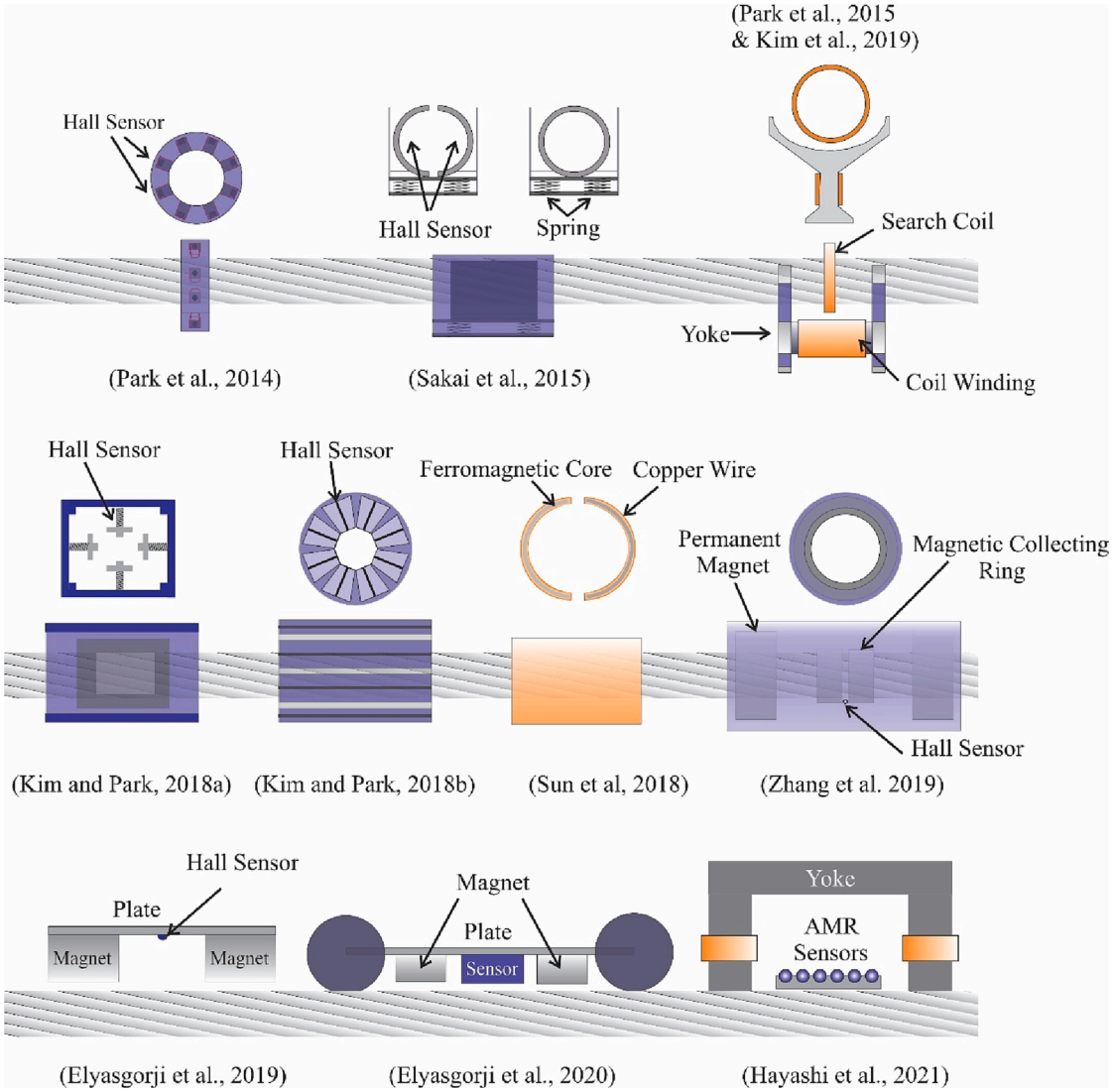

Fig. 22. Damage detection apparatuses based on MFL.

damage width increases. Third, to quantify the damage depth and width, a two-stage ANN classifier was designed, which was able to estimate the depth in the first stage and identify width in the second stage, as seen in Fig. 23.

Zhang *et al.* [69] utilized a micro-magnetic sensor to measure the self-magnetic field leakage (SMFL) signals stimulated by Earth's magnetic field and caused by corrosion or stress concentration in rebars. Plotting the tangential field (*Hx*) distributions at different lift-off heights, they found that the distance between these intersections was almost equal to the length of the corrosion region, especially in old corrosions. Xia *et al.* [70] enhanced this method by quantifying the corrosion's severity. They applied a combined horizontal and vertical scanning to determine the x-z curve reflecting the degrees of corrosion as well as the range of corroded area in unstressed strands. Considering the trapezoidal corrosion section, the curves indicate an inverted U-shape, as shown in Fig. 24, whose maximum value increases as the corrosion time goes on. They verified the experimental results through a theoretic magnetic dipole model and Faraday's first law of electrolysis. Mosharafi, et al. [71] proposed a passive method for corrosion detection in concrete rebars and investigated self-magnetic behavior through numerical and experimental data recorded by iCaMM device. It was shown that there are identifiable differences between the standard deviation, mean, frequency content and trend of recorded magnetic flux density of intact and corroded rebars.

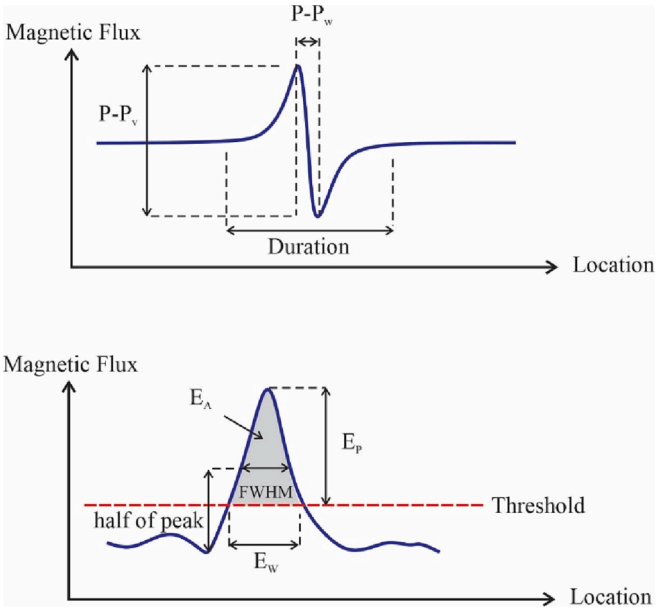

Fig. 23. Damage indexes for MFL signal.

Sun *et al.* [72] proposed the open EM flux leakage device shown in Fig. 21, which can be applied for damage detection of wire ropes and rebar structures. The device includes a C-shaped ferrous core, covered with a C-shaped loop-coil, and a Hall-array sensor to record leakage signals. Unlike the traditional tubular (cylindrical) coils, it can encircle rebars without head and tail. It was observed that the open magnetized coil possesses a stronger magnetic field and an excellent defect-detection capability than tubular coils. Zhang *et al.* [73] applied the circumferential multi-circuit permanent magnet exciter (CMPME), drawn in Fig. 21, to excite wire ropes more easily and uniformly. They installed a magnetic concentrator to increase the angular sensitivity range of Hall sensors, reduce the number of involved sensors, and thereby simplifying the signal processing task. Elyasigorji *et al.* [74] fabricated an MFL apparatus with two DC permanent magnets connected and a steel plate, placed a Hall sensor between the magnets, as seen in Fig. 21. It was demonstrated that peak-to-peak index and duration index increase when the percentage loss is increased. These indexes are illustrated in Fig. 22. Elyasgorji *et al.* [75] extended the previous research [74] and considered the effects of steel shear reinforcement (stirrups) using the device shown in Fig. 21. The moving MFL apparatus developed at the University of Wisconsin-Milwaukee [76], consisting of two DC permanent magnets and 64 axial longitudinal and vertical Hall sensors, was passed along the length of strands. They utilized correlation analysis to identify the location of stirrups, and then their effects were removed from the measured signals to discover damage locations. Azari *et al.* [77] developed a robotic system that includes two magnets, an array of MSs, and a robotic rover crawling along the I-girders of a prestressed concrete bridge. The system should not be employed on severely spalled and indented surfaces, since rough surfaces obstruct the smooth movement of the robot and thereby inducing confusing signals. Hayashi *et al.* [78] proposed unsaturated AC magnetic flux leakage (USAC-MFL) that uses an alternating magnetic field without the need for a strong applied magnetic field compared to the conventional MFL methods. A schematic of this device can be seen in Fig. 21. Considering various lift-offs and crack locations, they compared the distribution of magnetic fields. The sensor array was able to detect the change in the field distribution caused by the cracks, but there was no difference in the case of half-crack rebar when the location of the crack was different. Mujika *et al.* [79] utilized the inspection of trends of integrity and operation system, consisting of an arrangement of MFL, tool movement, magnet, and caliper sensors for inspection of 23.9 km of a Colombian gas pipeline. First, weld points were detected using windowed overlapping root mean square of all MFL signals, to update the weld chart. Second, to find damages, sections whose recorded variables behaved differently than the mean were detected, in terms of Q and T^2 statistical indices obtained by applying PCA.

As listed in Table 6, in this section some of the most important articles that applied MFL for damage detection are reviewed. This method is mostly used for detecting cross-sectional damage in elongated ferromagnetic materials, such as fracture and corrosion in steel cables, and wire ropes. The magnetizer used in MFL techniques plays an important role in stimulating the ferromagnetic structures. They can be electromagnets [65,66,72] or permanent ones [67,73–75], each of which has its own advantages and shortcomings. Electromagnets, unlike permanent ones, are adjustable, but they need an energy source, and they produce heat that should be cooled via heat dissipation tools. Although some of the research studies considered self-magnetism, their application was limited to unstressed strands. To measure MFL, Hall sensors are used more than others [62,64,67,72–75], whereas other types of sensors, such as MR [64], AMR [78], and search coils [65,66], are utilized occasionally. The measured raw signals usually need to be denoised or processed for ease of anomaly detection through a low-pass filter, offset correction and Hilbert [67] or fast Fourier transform [78]. In order to detect and quantify the damage objectively and automatedly, thresholding [62,67], feature extraction [67,68,74], regression [65,67], and machine learning methods [68] are used. An MFL apparatus can move along the structure at a constant speed and inspect the structure. In most

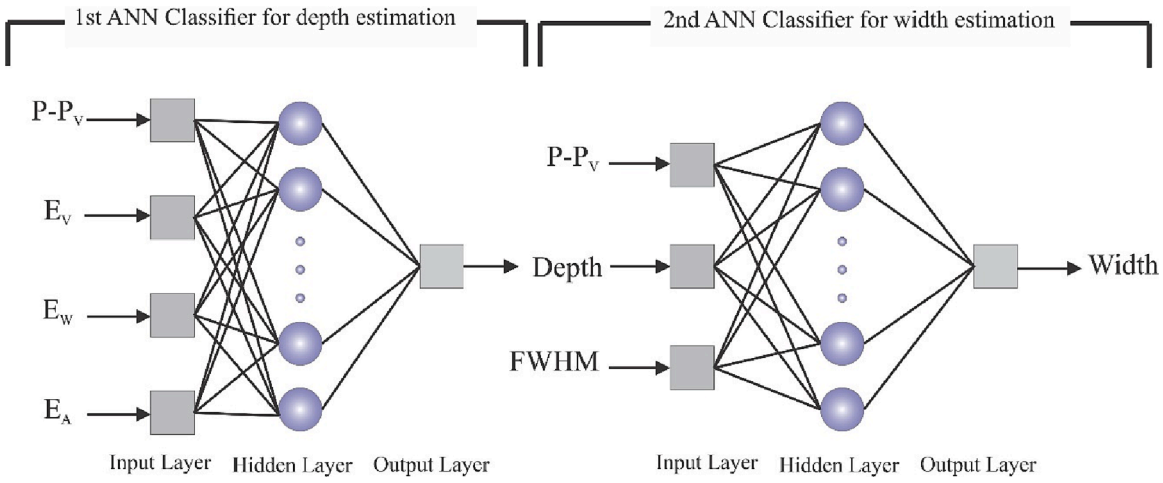

Fig. 24. The architecture of the ANN used for estimation of different characteristics of damage.

Table 6
Types of structures and damages examined by the MFL method.

Reference	Year	Damage type, application and main features
Park, et al. [62]	2014	Cross-sectional loss of steel cables - Accurate method - Not requiring an expert - Light weight - Not requiring any power for magnetization
Sun, et al. [63]	2015	Cross-sectional loss of steel cables - High resolution - High sensitivity - Fast computation - Real-time - High SNR - Reliable - Causing less wear and damage - Small size and light weight
Sakai, et al. [64]	2015	Back-side corrosions of steel plates - Requiring minimal labor - High sensitivity - Fast measurement
Park, et al. [65]	2015	Cross-sectional loss of steel cables - Low-pass filtering and DC drift correction for high resolution
Kim and Park [67]	2018	Cross-sectional loss of steel cables - Less error compared with P-P index. - Real-time - No power required for magnetization - Light weight
Zhang, et al. [69]	2016	Corrosion of rebars - Easy and fast operation - Inexpensive - Using Earth's magnetic field
Sun, et al. [72]	2018	- Consuming more electric energy - The rebar should be ferromagnetic - Real-time - Suitable for elongated objects without heads and tails
Kim and Park [68]	2018	Cross-sectional loss of steel cables - Error is close to zero - Reliable - Real-time - Non-contact
Zhang, et al. [73]	2019	- High sensitivity - Accurate and reliabe - Real-time
Kim, et al. [66]	2019	Cross-sectional loss of steel cables - A cross-sectional loss of less than 2% can be detected - Reliable
Xia, et al. [70]	2019	- The error does not exceed 5%.
Elyasigorji, et al. [74]	2019	Corrosion of PSC tendons - Reliable - Cost-effective - Time-saving
Elyasigorji, et al. [75]	2020	Corrosion of PSC tendons - A cross-sectional loss of less than 2.4% can be detected
Mosharafi, et al. [71]	2020	Corrosion of rebars - Time and cost effective
Azari, et al. [77]	2020	Corrosion of rebars - Near real time - High sensitivity - High SNR - Linear performance
Hayashi, et al. [78]	2021	Fracture of rebars - Covering a wide scanning range - Time-effective - Reduced labor - Applicable at high lift-off conditions - Low power consumption
Mujica, et al. [79]	2021	Welding and abnormal condition of pipes - Unable to identify the type of damage - Capable of traveling inside pipelines - Demanding high-capacity memory

studies, the MFL technique is used for elongated objects such as rebars, and cables, although there are few studies investigating plates [64] and pipelines [79]. The apparatus should be tailored to the operational condition, for example, some studies investigating the rebars, such as Ref. [72], cannot function for rebars inside the slabs or beams due to shape incompatibilities. MFL is prone to misdetections caused by sudden operational movements, large distances between the sensors and the object [62], Signal-to-noise ratio (SNR) [67], welding [79], stirrups [75,77], edges [63], etc.

2.7. Magneto-Mechanical sensors

In this technique, a Magneto-Elastic Active Sensor (MEAS) is applied for generation of elastic waves via eddy current. MEAS consists of a coil, initiating eddy currents within metallic structure, and a permanent magnet above the coil, generating the elastic wave via Lorentz force in nonferromagnetic metals. As seen in Fig. 25, the magnetic induction field, shown in red, extends into the metallic element. The electricity in the coil induces eddy current whose mutual orientation with the magnetic induction produces Lorentz force transferred to lattice ions. The force initiates both longitudinal and flexural elastic waves exciting thin-walled metallic structures. The waves travel in the structure and produce modal spatial patterns at respective resonance frequencies. It has been indicated that the electrical impedance response of the sensor reflects local mechanical changes (defects) in the structure [80]. In other words, MEAS excites vibrations in the structure and simultaneously the vibrations reflect themselves in the impedance response.

Zagrai and Çakan [81] tested the structural diagnostic capabilities of the Magneto-Mechanical Impedance (MMI) technique on different samples, including honeycomb panel, adhesive joints, bolted joints and large panels with simulated cracks. They observed that deteriorations in bonds and loosening of the bolts and cracks can manifest themselves in alterations in the position and amplitude of the peaks of the impedance responses. The sensor can be applied in physical contact or non-contact modes with the test structure. Doyle, et al. [82] investigated the diagnostic capabilities of MMI for bolt loosening. It was observed that removing and placing back the sensor does not make significant change in the resultant impedance. Additionally, as the bolts are loosened, the peaks and energy densities shift downward to lower frequencies. Zagrai and Çakan [83] showed that the excitation of vibration modes depends on the MEAS position in physical contact mode. It was demonstrated that the impedance response can be improved by adding further turns in the coil, using stronger magnets, and reducing the lift-off gap between the sensor and the test element. It was also concluded that since the elastic wave occurs in surface-adjacent volume, it can be applied to damage identification in thin layers and high-temperature non-contact assessments. Shuai and Tang [84,85] formulated a mathematical model describing the sensor-structure interaction and impedance response with a given lift-off distance. According to their conducted experiments, the new model can accurately predict the peak values and their corresponding frequencies. Roskosz and Fryczowski [86] conducted an analysis on determining the active stress in steel elements by measuring different magnetic methods, including two active methods - Barkhausen noise and impedance in in-series LCR circuits (consisting of an inductor (L), capacitor (C) and resistor (R)) - and a passive method - residual magnetic field (RMF) components. The Barkhausen effect and RMF components are only usable for ferromagnetic or austenitic steels, while the impedance parameter can be applied for all steel grades and even for Al- and Cu-alloys. It was indicated that stresses can be identified using the parameters of the Barkhausen noise quantity, and stresses correlate with the impedance frequencies. But the RMF components do not correlate with the stresses resulting from more than one cycle of loading. Due to the magneto-mechanical phenomenon, change in stress condition of ferromagnetic elements can change the material magnetization intensity. Szulim and Gontarz [87] studied changes in magnetic fields to assess the stress condition of steel samples. They observed that the stress

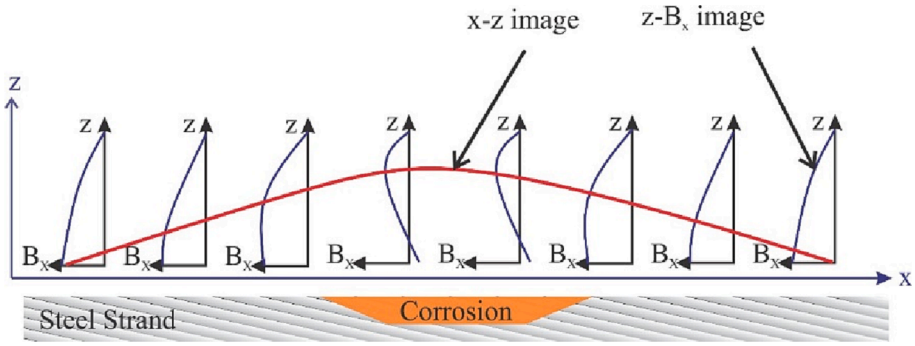

Fig. 25. Diagram of an x-z image produced by scanning a corroded steel strand.

state of the material in the elastic zone can be identified by spatial fluctuations of the magnetic field, but in the plastic zone the fluctuations were considerably smaller.

A summary of the reviewed papers in this section are provided in Table 7.

2.8. Magnetostrictive sensors

Al-Hajjeh, et al. [88] fabricated a stress sensor based on Villari effect (inverse magnetostriction) using a magnetostrictive composite material (MCM) and epoxy resin. Due to the effect of external mechanical stress magnetic domains in the MCM expands, which can be estimated through measuring inductance probe, as shown in Fig. 26. The sensor can be used for determining defects as well as the stress vector – magnitude and direction – in steel structures.

Fang and Tse [89] presented a kind of magnetostrictive transducer with axial magnetized patch for defect detection in concrete-covered pipe risers, as shown in Fig. 27(a). It was shown both theoretically and experimentally that higher signal amplitudes can be obtained using magnetized iron cobalt patch and larger length–width ratios. Also, the axial magnetized transducer works better than the ordinary version in terms of reduced energy leakage and distinguishability of the end echo. Fang and Tse [90] developed a similar technique for determining the axial and circumferential location of damage in small-diameter pipes (Fig. 27(b)). Six thin films of flexibly printed circuits were pasted around a sheet of magnetostrictive material to generate axial dynamic magnetic field, and consequently induce normal strain via the Joule effect. When a defect occurs in the pipe, there will be echoes that can be used for detecting its location. Although the results were satisfying, it encounters many challenges, such as low detectability of small cracks, especially in presence of multiple cracks; and significant discrepancies between the numerical and experimental models.

Gullapalli, et al. [91] proposed a method for strain sensing in fiber-reinforced composites. They used inkjet-printed copper induction coils, as senors, with hand-wound coils and AMR sensor. In addition, two different forms of actuators, including FiSiB ribbon cocured onto the surface of composite and magnetic particles impregnated into epoxy. It was observed that inductance generally decreases with decrease in strain. The best reponse was acquired by FiSiB as acutator and 10-turn monofilar inkjet-printed sensors.

The details regarding the reviewed references are provided in Table 8.

Table 7
Summary of the studies on magneto-mechanical sensors.

Reference	Year	Damage type, application and main features
Zagrai and Çakan [81]	2008	Disbond joints, cracks, and loose bolts of metal structures - Suitable for high-temperature non-contact applications - Suitable for through-paint and dirt inspection - High accuracy - High SNR
Doyle, et al. [82]	2009	Disbond joints, cracks, and loose bolts of metal structures- In low frequencies (1–10 kHz), it can be applied in a non-contact way - Real time - Long wavelength of elastic waves limits the detection capability to the sensor near-field.
Zagrai and Çakan [83]	2010	Disbond joints, cracks, and loose bolts of metal structures - Suitable for high-temperature non-contact applications - Suitable for through-paint and dirt inspection - High SNR
Shuai and Tang [84,85]	2013	Change in thickness of electrically conductive structures - Real-time - Non-contact
Roskosz and Fryczowski [86]	2020	Stress in steel structures - Quantitative relations between applied stresses and the Barkhausen noise
Szulim and Gontarz [87]	2021	Stress in steel structures - Requiring movement of the object in relation to the magnetic field - Predicting the plastic range - High accuracy

2.9. Magnetic microwire sensors

In this section, a sensor is introduced that can use magnetic properties to detect stresses applied to non-ferromagnetic structures. Magnetic microwires (MM), usually made by the Taylor-Ulitovski method, have a very thin ferromagnetic core covered with a layer of glass (Fig. 28). This component is placed inside composites or any material whose stress measurement is required. Next, a magnetic field moving coil is employed to apply a magnetic field to the microwire, and the field is felt near this microwire by a sensor coil. By applying stress to the composite, and consequently to the microwire, a change in the magnetic properties occurs that results in a change in the sensor coil signals.

Olivera, et al. [92] proposed a magnetic microwire embedded in cement-based composite (MMCC) that is able to monitor stress variations in concrete by means of EM induction (Fig. 29). The MMCC was equipped with pick-up and excitation coils protected with Teflon, and a digital oscilloscope captured the output of pickup coil. It was shown that compressive stress has an inverse relation with both peak position and peak amplitude, but the peak position exhibits significantly higher deviation in higher compressive stresses (larger than 18 MPa).

Atalay, et al. [93] performed experiments on FeSiB amorphous magnetic wire by changing the annealing time and investigating the magnetic properties, such as resonance frequency and amplitude under DC exciting magnetic field produced by a magnetoelastic sensor (two-wire winding as exciting and pick up coils). They found some relationships between annealing time and magnetic property, and investigated resonance frequency and amplitude in a constant magnetic field with a

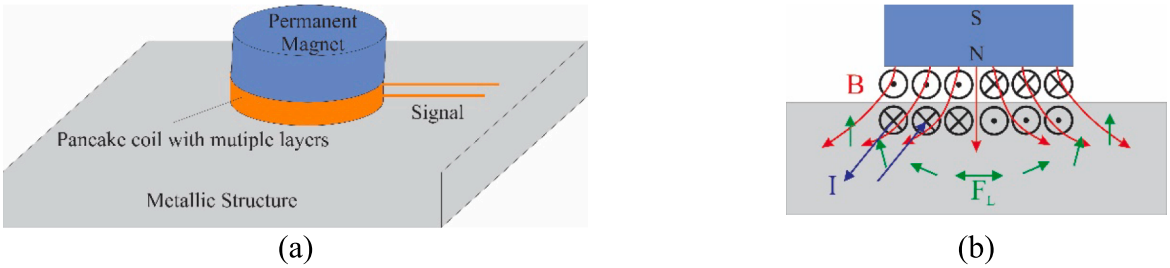

Fig. 26. Electro-mechanical sensor: (a). A schematic of the sensor, (b). Interaction of the coil and structure.

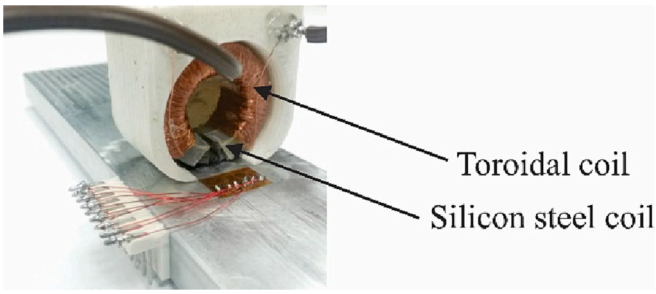

Fig. 27. The MCM sensor (taken from [88]).

Table 8
Types of structures and damages examined by magnetostrictive method.

Reference	Year	Damage type, application and main features
Al-Hajjeh, et al. [88]	2016	Stress in aluminum substrates - Easy operation in the field because of wireless coupling between the sensors and probe - Low cost
Fang and Tse [89]	2018	Defect in steel pipes - The static magnetic field intensity should be controlled in a suitable range - The more the length–width ratio, the higher the maximal magnetic field intensity - Robust against noise and suitable for concrete-covered riser defect identification
Fang and Tse [90]	2019	Defect in steel pipes - Determining the axial location and circumferential orientation of defects - High efficiency - Low cost - Good control over wavelength - Real-time - Small size - Easy installation
Gullapalli, et al. [91]	2021	Strain in composites - High accuracy - High sensitivity - Real-time - Low-cost and easy fabrication - Light weight - Large surface area

magnetic wire. It was indicated that the magnetic wire can detect the viscosity of the media.

Churyukanova, et al. [94] presented an experiment on tensile force measurement in composite through Fe-based magnetic microwires and developed an experimental setup as shown in Fig. 30. By applying stress to microwire, it changed magnetostriction coefficient and measured Barkhausen effect. The picking-up coil detected this effect and changed the magnetic property by variation of EM induction, resulting from change in the pick-up coil's voltage amplitude.

Olivera, et al. [95] developed a pressure measuring system, using three magnetic microwires, a commercial strain gauge embedded inside the concrete, a pick-up coil, and an exciting coil outside the concrete. They validated the results of MM sensor, comparing its results with those of a strain gauge. Ali et al. (2021) [96,97] applied a bistable magnetic microwire to measure strain in a beech plywood strip. To detect the switching field and transform it into a sensing signal, a pickup coil was attached near the microwire. It was observed that there is almost a linear dependence between the switching field and applied stresses. The small size of the sensor makes it possible to be applied for constructing self-monitoring smart plywood.

Table 9 summarizes the reviews provided for the microwire sensors.

2.10. Smart rocks

The measurement of the scour depth around bridge piers and abutment corners is difficult during flood event. During such harsh situations, it is critical to monitor scour depth and prevent scour-induced collapses of infrastructures. Chen, et al. [98] proposed a methodology to embed permanent magnets in acrylic balls – smart rocks – and integrate them with the process of scouring. The applicability of most of the existing technologies is limited in terms of accuracy, however, smart rock seems a promising method to timely warn the users and owners during such situations and in real-time. When the smart rocks fall into the bottom of scour hole, the maximum scour depth can be determined with a magnetometer. They showed that the sensitivity of smart rocks to the change in the hole is sufficient for the monitoring process. The method is remarkably cost-effective that can also be applied in other vulnerable places, such as dams, river banks, and levees. The spatial localization of smart rocks is a critical problem in this method yet to be addressed.

Tang, et al. [99] proposed and validated two types of smart rocks, including Arbitrarily Orientated System (AOS) and Automatically Pointing to South System (APSS), for bridge scour monitoring. APSS involves a sophisticated configuration and is automatically pointing to the south geomagnetic pole of the Earth. In addition, an effective algorithm was devised to localize the position of smart rocks by minimizing the difference between the measured and estimated location. Fig. 31 illustrates a schematic of the field application of them for scour monitoring. They observed that the localization error of the APSS is less than $0.1m$ and the algorithm's computation time is in the order of a few seconds. The maximum scour depth for effective monitoring using the tested smart rock was limited to $12.1m$. Fig. 32.Fig. 33..

Zhang, et al. [100] applied the Unmanned Aerial Vehicle (UAV), equipped with a high-resolution magnetometer and GPS, as a mobile station to measure the magnetic fields of smart rocks for scour monitoring. Unlike the previous studies which required blocking traffic, the proposed approach did not need any traffic control during inspection, and led to competitive results. They concluded that the UAV and steel used in bridge structures – steel girders and bars – cause magnetic inference when they are placed in the proximity of the magnetometer. Additionally, to limit the dynamic effects, the fly speed of the UAV should not exceed $2m/s$.

The reviews provided for the smart rocks are summarized in Table 10.

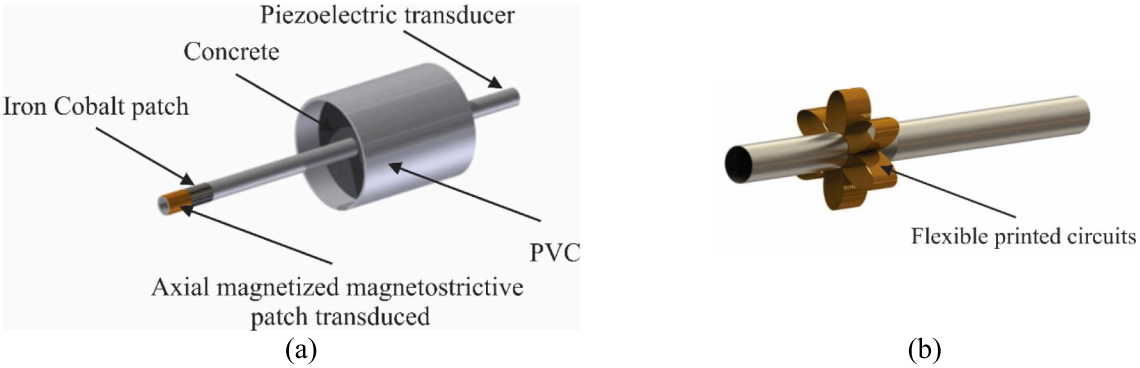

Fig. 28. Magnetostrictive patch transducers: (a) axial magnetized (b) segmented axially magnetized (taken from [89;90]).

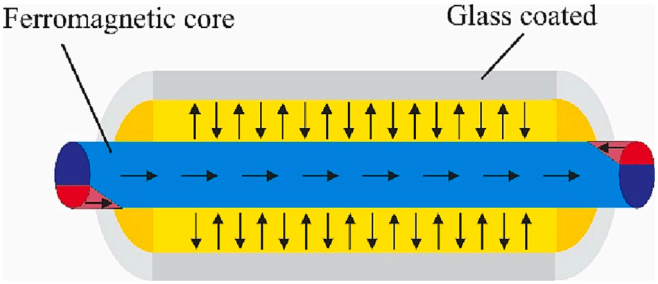

Fig. 29. Schematic of a magnetic microwire.

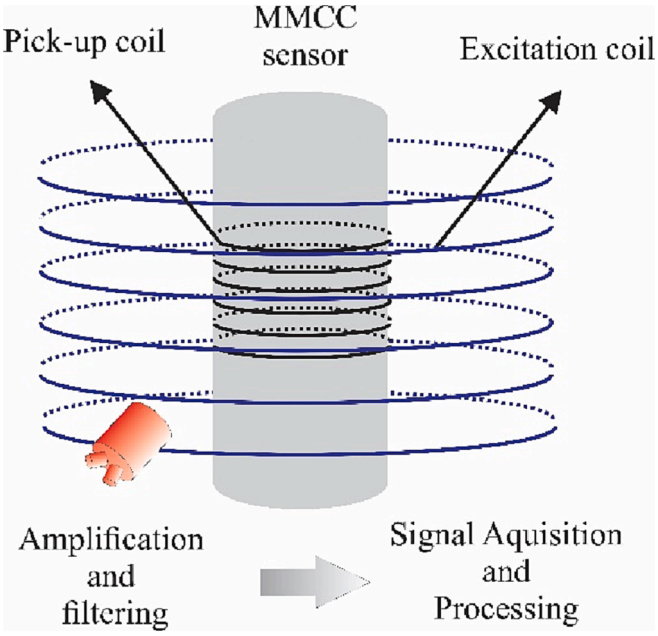

Fig. 30. The schematic of MMCC sensors.

Table 9
Types of structures and damages examined by magnetic microwire sensors.

Reference	Year	Damage type, application and main features
Olivera, et al. [92]	2014	Tensile force in concrete structures - Contacless excitation and pick-up coils
Atalay, et al. [93]	2016	Viscosity in liquids - Small size - High sensitivity
Churyukanova, et al. [94]	2018	Tensile force in composites - High stress sensitivity
Olivera, et al. [95]	2019	Stress in concrete structures - Small size - Light weight - High sensitivity - Fast production - Low cost - Contactless - Very fast
Ali et al. [96,97]	2021	Strain in beech plywood - High sensitivity - Small size - Possibility for contactless monitoring

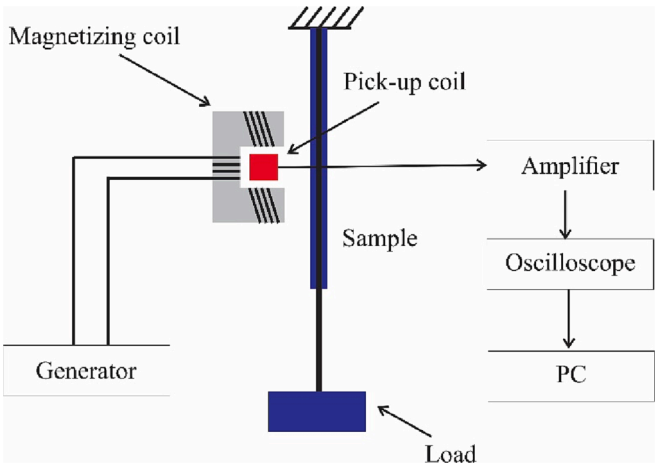

Fig. 31. The scheme of experimental setup.

2.11. Other magnetic sensors

Zhixiang, et al. [101] proposed a smart film with MSs for surface crack monitoring in concrete bridges. To reduce the fragility and expensiveness of the common smart films, they replaced silver wire and resin film by magnetic enameled copper wire and self-adhesive plastic film, respectively. After adhering the wires on the structure, the plastic film was peeled off, and the on–off signals could signify cracks. The mechanical and electrical durability of the smart film were analyzed, and it was indicated that it can preserve its performance when cracks appear. A real-world application of the smart film is shown in Fig. 34. The smart film can cover and monitor entire area of the critical zones in structures. The cover might have benefits regarding preventing from propagation of the cracks. The method is limited to surface cracks, and subsurface cracks cannot be monitored. The performance of the method still needs to be investigated under harsh chemical and environmental conditions, such as PH variation and raining. In future studies, one may also consider the optimal orientation of wires considering the elements

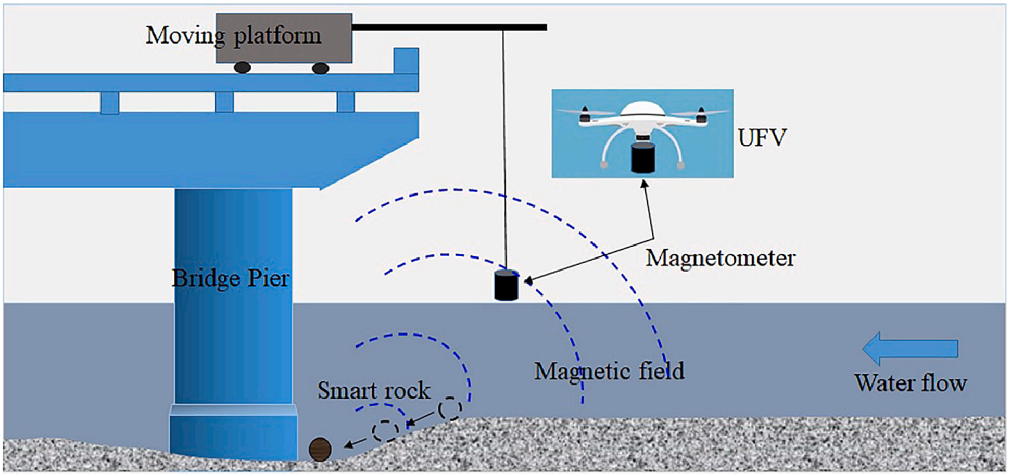

Fig. 32. An illustration of application of smart rocks for bridge scour monitoring [2].

Fig. 33. Smart film used on Taipingzhuang bridge (taken from [101]).

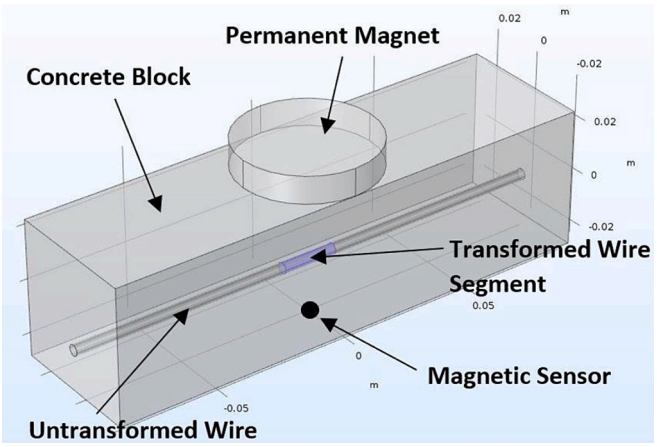

Fig. 34. An illustration of the application of MSMA wire in a concrete beam (taken from [104]).

Table 10
Types of structures and damages examined by smart rocks.

Reference	Year	Damage type, application and main features
Chen, et al. [98]	2014	Scour depth in bridge piers - Real-time
Tang, et al. [99]	2019	Scour depth in bridge piers - Low error - Able to trace the trajectory of smart rock.
Zhang, et al. [100]	2021	Scour depth in bridge piers - Real-time

to be monitored.

Kurz, et al. [102] applied micromagnetic sensors for long-term structural health monitoring (SHM) in stay cables of a real bridge in Germany. Both the maximum Barkhausen noise amplitude and the harmonic distortion factors featured a 50% size effect. The results demonstrated that changes in load and breaks in wires clearly correlate with signal peaks recorded by the sensors. However, the method requires an objective signal processing system to identify and interpret signal changes. Kypris and Markham [103] developed a low-frequency magnetic system to measure 3D displacements within concrete. They used three mutually-perpendicular coils at both transmitter and receiver sides, whose relative displacement can be estimated by optimizing the magnetic field distribution model against the measured data. Since dielectric media – such as concrete, soil and water – are transparent to low-frequency magnetic fields, the system can be embedded inside concrete structures. In Table 11, the maximum range, degree of freedom, resolution, and linearity (with respect to the full-scale output) of the designed sensor are compared with other popular position measurement sensors gathered in ref. [103].

Davis, et al. [104] embedded magnetic shape memory alloys (MSMA) inside concrete beams and investigated their application in SHM. As seen in Fig. 35, the model consists of a permanent magnet on one side of the beam, a MS (probe) on the opposite side, and an MSMA wire in between. Under bending, a localized phase change occurs in MSMS and alters the magnetic field lines, which is detected by MS. Both the numerical and experimental results indicated that there is a significant correlation between the cross-sectional area of MSMA and the magnetic field strength.

Pospisil, et al. [105] applied metal magnetic memory technique and utilized magnetometer data to diagnose magnetic field strength in concrete rebars and locate their missing parts. The magnetogram data and its gradient were derived in both contacted and contactless states with 50 mm distance from the surface. The zones with missing reinforcing were detectable with an increase in gradient. The method is prone to false positive detection because the residual magnetization of a material may stem from factors other than damage, such as production process, machining, cutting, welding, bending, heat treatment, cooling, and operational stresses. Yin, et al. [106] showed that there is a high correlation between the magnetic induction intensity and load intensity of concrete samples because of piezoelectric, crack propagation, and

Table 11
Comparison among different commercial position measurement sensors.

Sensor	Maximum Range	Resolution	Linearity	Degree of Freedom
Capacitative				
CapaNCDT 6110	10 mm	0.01%	± 0.05%	1-D
Capteura 250 Series System	2.5 mm	0.0015%	± 0.05%	1-D
Eddy Current				
eddyNCDT 3001	4 mm	0.1%	± 0.7%	1-D
ECL202	15 mm	0.01%	± 0.2%	1-D
Inductive				
induSENSOR VIP series	150 mm	0.03%	± 0.25%	1-D
BIP 103	103 mm	0.08%	± 0.4%	1-D
EX-500 series	10 mm	0.03%	± 0.3%	1-D
ECL202	15 mm	0.002% − 0.009%	± 0.2%	1-D
Magneto-inductive				
mainSENSOR	55 mm	<0.05%	< ±3%	1-D
BIL 60	60 mm	0.0003%	± 1.67%	1-D
RFID				
RFID displacement sensor (MIT)	40 mm	6.2%	Unreported	1-D
RFID displacement sensor (TU Darmstadt)	4 mm	6%	Unreported	2-D
Low-frequency magnetic				
Kypris and Markham [103]	50 mm	0.5%	± 3.5%	3-D

friction effects in different stages. According to the phenomenon, they designed a non-contact MS, by which linear elastic, plastic and failure stages of the loading were distinguishable. Nazar, et al. [107] conducted numerical and experimental studies on crack identification of steel plates deploying smartphone magnetometer sensor. In order to enhance the magnetic field, four Neodymium magnets were installed on the plate. The results showed that as the crack progresses the magnetic field intensity increases; therefore, cracks can be identified through tracking changes of the magnetic field. The method is cost-effective, but it loses its accuracy when the distance increases and its application in the detection of cracks in different orientations need to be studied. To detect internal corrosion in ferromagnetic pipelines, a sensor consisting of a strong permanent magnet, a Fiber Bragg Grating (FBG) strain sensor and a non-magnetic material was developed [108,109]. Corrosion in the pipe decreases the thickness of its wall, and consequently, the magnetic attraction force between the wall and the magnet decreases. A sensor attached to the pipe can monitor the strain changes caused by magnetostatic force acting on the magnet. Shiryayev, et al. [110] designed two variations of this sensor, as presented in Fig. 34. In the first version (Fig. 34 (a)), the magnet was encased in a ferromagnetic enclosure, and the second version (Fig. 34 (b)) included a magnetic counterbalance placed on the opposite side of the first magnet. It was observed that the first case provides larger magnitudes of the force and the second case improves the sensitivity of the sensor. Additionally, finetuning the position of the magnet near the equilibrium state can improve the sensitivity of the sensor.

Lei, et al. [111] numerically analyzed the performance of Magnetic Corrosion Detector (MCD) in quantitative monitoring of the corrosion process of steel rebars in concrete structures. MCD works based on the magnetic medium theory, relating the induction intensity change around a corroded steel to its geometric change caused by corrosion. It was indicated that the corrosion can be estimated through a linear relation between the corrosion and the voltage reduction measured by the device. However, the steel rebar should be placed right at the center of the test area for higher accuracy.

Powering of wireless sensors is another advantage of MSs. Although radio-frequency techniques have reduced the need for wired monitoring systems, the power supply is a serious challenge yet to be solved. Andringa, et al. [112] proposed an unpowered wireless corrosion sensor to detect the extent of corrosion in reinforced concrete. The sensor is hermetically sealed and involves an inductive coil of wire magnetically coupled to a reader coil outside the structure which powers and interrogates the sensor. Studying the impedance through the reader inductor, it was shown that the resonance of the sensor is detectable as a dip in the phase curve, and the corrosion manifests itself in increasing the resistance and shifting the frequency. Additionally, it was indicated that a pseudo-quality factor calculated by Eq. (1) can be adopted as a more informative feature for NDE.

$$Q = \frac{\omega_0}{\Delta\omega} \tag{1}$$

where, ω_0 is the resonant frequency of the sensor and $\Delta\omega$ is the width of resonance, derived from the phase response of the reader. The method needs to be investigated in long-term corrosions and when the structure is exposed to other corrosive materials. Kim, et al. [113] developed a magnetic resonance-based wireless power transmission (MR-WPT) system (shown in Fig. 35) that can supply large amount of energy whenever it is needed and without sharp degradation of power transmission efficiency (PTE) despite the increase of transmission distance. They showed that the existence of concrete structure improves PTE compared with air because of paramagnetic properties of cement, but the PTE of reinforced concrete is 3% lower than that of unreinforced concrete.

Lu, et al. [114] proposed a local, mechanical rail-mounted energy harvester based on EM-induction principle to power wireless

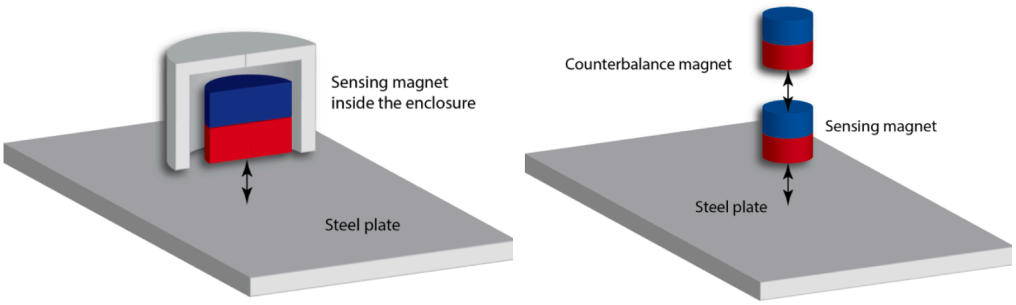

(a) Configuration with a magnet inside an enclosure.

(b) Configuration with sensing and counterbalance magnets

Fig. 35. Two conceptual configurations of MSs (taken from [110]).

rechargeable sensor nodes. As shown in Fig. 36, the harvesting system contains a suspended magnet placed inside a tube of copper-made coil and between a couple of top and bottom repelling magnets. Further studies in energy harvesting for railway applications can be found in [115,116].Fig. 37..

Since the WPT through obstacles can be challenging due to penetration, reflection and attenuation, Wang and Markham [117] considered the fact that almost all structural concretes are reinforced with steel, and the rebars can act as a magnetic conduit for low-frequency magneto-inductive fields. They applied a constant phase element (CPE) to simulate the complex multi-coupled physics mechanisms. Despite the losses in the rebar path (because of the resistance in CPE), the method possesses higher coupling compared to air, especially at long distances. Therefore, sufficient amounts of power can be harvested at large distances by employing intermediate sensors acting as resonators along the rebar. The method can be utilized for energy supply and probably information communication for embedded sensors.

Furkan, et al. [118] transformed a suit of wired sensors into wireless units to confirm their laboratory and field applications. Among their sensors, six magnetic strain gauges were verified, where the friction between the steel surface and gauges was leveraged by a magnet. This connection accelerated the installation and removal operations compared with welding and adhesives.

Table 12 summarizes the reviews provided for the MSs in this section.

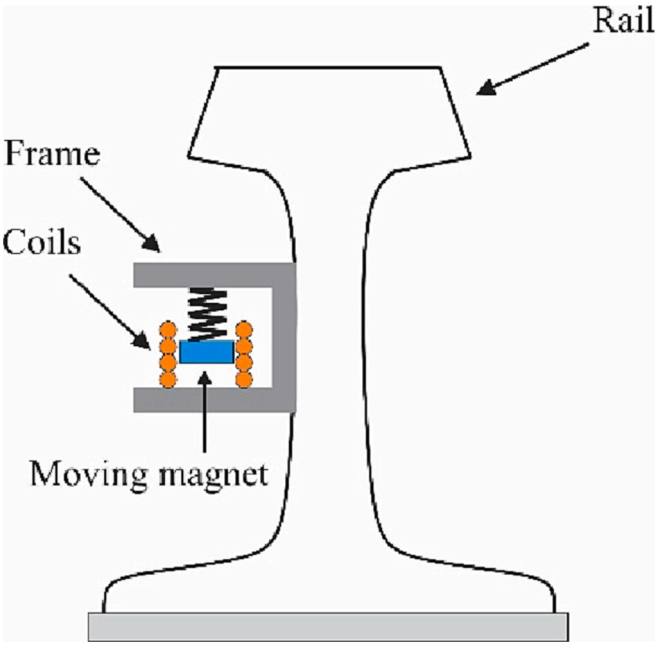

Fig. 37. The physical model of the energy harvester.

3. Conclusions and future research directions

In the present paper, the applications of MSs in NDE of civil engineering applications are overviewed. The sensors provide a wide spectrum of applicability from load detection to corrosion monitoring. MSs provide reasonably cheap solutions that can expedite the NDE process. Their low power consumption, high sensitivity and small size provide opportunities for green and sustainable sensing and pave the way for IoT and smart structures.

While the accelerometers must be firmly attached to structures near the vibration sources, the MSs can be employed in a dynamic fashion through robots, thereby covering a large area. Additionally, because of the penetration capability of the magnetic field, inner damages and corrosions can be identified by this type of sensor which is a key advantage compared to vision-based techniques.

When choosing an MS for a specific application, it is important to carefully consider the advantages and disadvantages of each type of sensor.

Hall effect sensors are a cost-effective option and can be conveniently integrated into monitoring systems. They are compact in size and consume minimal power, making them a suitable choice for wireless corrosion detection in reinforced concrete structures. However, it is important to note that their performance is adversely impacted by noise and environmental factors like temperature changes. Unlike, Hall effect sensors, which are inexpensive, MR sensors are rather expensive. But they can provide an SNR at least 10 times higher than that of Hall effect sensors, as well as a 100 times higher field resolution.

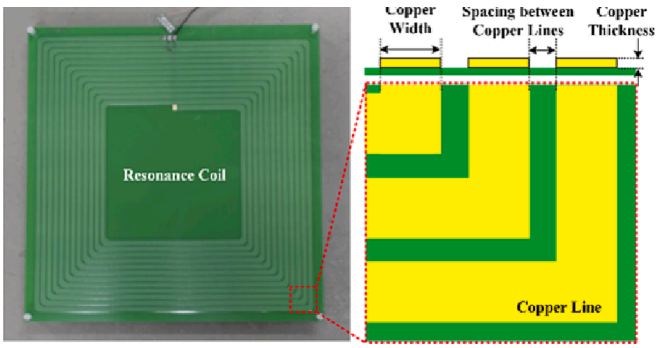

Fig. 36. The fabricated spiral type resonance coil (taken from [113]).

EM sensors offer a wide frequency range for monitoring structures, such as detecting rebars in reinforced concrete structures. Nevertheless, they are sensitive to environmental interferences, such as nearby electrical equipment or magnetic fields generated by other sources. Further, unlike Hall effect sensors, they usually require significant power for operation, which means that they are not suitable for use in remote locations or in situations where power is limited.

For detecting subsurface defects in steel structures, MR and eddy current sensors are commonly used. Eddy current sensors are proper for measuring non-ferrous materials like aluminum and offer durability and resistance to environmental factors. On the other hand, MR sensors have a higher sensitivity to small variations in magnetic fields, are smaller in size, and have lower power consumption compared to eddy current sensors.

For detecting cross-sectional loss in cables, MFL sensors are preferred as they are fast, efficient, and non-contact, and provide high-resolution images of the cable's internal structure. Magnetoelastic sensors are ideal for measuring very small changes in magnetic fields, making them a great option for measuring forces in cables. They are also durable and can withstand harsh environmental conditions. On the other hand, magnetostrictive sensors offer real-time monitoring of steel pipes and are cost-effective. However, they have challenges in detecting small cracks.

For monitoring structures with many bolts like steel bridges, magneto-mechanical sensors are a suitable choice as they can be installed quickly and provide real-time assessment of bolt loosening. They are also robust against noise and require minimum power consumption. For monitoring scour, smart rocks provide cost-effective real-time monitoring but may be limited in size and potential interferences from other magnetic materials.

The choice between these sensors is dependent on the required application. Enhanced accuracy and reliability can be obtained through their combination, which is almost neglected in the literature.

Although MSs received remarkable attention from the civil engineering community in recent years, there is still room for improvement. In the following, several challenges and prospects in this field are presented, upon which further studies and developments can be planned:

Table 12
Details of the reviewed papers.

Reference	Year	Damage type, application and main features
Andringa, et al. [112]	2005	Corrosion in reinforced concrete structures - Not requiring a battery within the sensor - Simple and inexpensive - Embedded in the concrete - Wireless
Altpeter, et al. [119]	2009	- The magnetic Barkhausen noise profile is influenced by the total stress state of the material
Zhixiang, et al. [101]	2010	Crack in concrete structures - Not able to detect subsurface cracks.
Kurz, et al. [102]	2013	Breaks in bridge cables - The resolution limit of the micromagnetic measurement should be approximately in the same order of magnitude as the traffic load.
Kim, et al. [113]	2015	Corrosion in reinforced concrete structures - Wireless - Not requiring a battery within the sensor
Kypris and Markham [103]	2017	3D Displacement in concrete structures - Low error - Able to measure position and strain at 3D
Davis, et al. [104]	2018	Crack in concrete structures - Low power consumption - Wide sensing range.
Lu, et al. [114]	2018	Corrugation of rail - Wireless - Not requiring a battery within the sensor
Wang and Markham [117]	2020	Corrosion in reinforced concrete structures - A long, flat coil transmits power more efficiently over long ranges, but a thick, short solenoid performs better over short ranges.
Furkan, et al. [118]	2020	Acceleration in aluminum beams - Lower error. - Short installation time and cost - Long service life - Accurate
Pospisil, et al. [105]	2021	Reinforcement condition in concrete structures - With a limitation in detection of reinforcement in steel ducts.
Yin, et al. [106]	2021	Failure of concrete structures - A good correlation between magnetic induction intensity and cumulative AE energy. - The more severe the damage is, the faster the cumulative AE energy increases.
Nazar, et al. [107]	2021	Crack in steel plates - Detection of limited pre-defined cracks.
Shiryayev, et al. [110]	2021	Internal corrosion of steel pipes - Magnet geometry with higher aspect ratio results in larger relative changes in the magnetostatic force.
Lei, et al. [111]	2022	Corrosion in concrete structures - The positioning error is about 5 mm. - The steel rebar should be placed right at the center of the test area - High error when corrosion ratio is very low.

- A magnetic shock can affect the output of most MSs (e.g., Hall effect, MR, eddy current, magnetoelastic, MFL, magneto-mechanical, magnetostrictive, magnetic microwire, and smart rock sensors) by an offset. Although it can be remedied through periodic magnetization, strong pulses should be avoided during instalment and application of the sensors.
- Fluxgates and MR sensors are prone to the Crossfield effect arising from magnetic fields perpendicular to the sensing direction – e.g., Earth's field. This issue can be addressed by feedback-compensated signal processing and magnetic anisotropy.
- Environment conditions such as temperature and humidity can influence the signals and performance of the MSs, especially Hall effect and magnetoelastic sensors. In this regard, appropriate temperature and humidity sensors as well as experimental results can be involved in the process to provide a calibration system and relevant correction factors to compensate for these effects.
- The magnetic fields exhibit sensitivity to element coating and geometry – e.g., thickness and element edge – which requires position-dependent calibration. Expanding on this topic is currently a vibrant area of research in the field of EM sensors.
- The loading history of materials can alter some of their magnetic properties, such as residual magnetic field, without occurring any damage. This shows the necessity of proper techniques and feature selection for specific applications, especially for MR sensors. The same goes for the material type of test structures.
- Most studies are just concentrated on the detection of damage presence or damage location. Various numerical, statistical and computational models can be developed to map the acquired signals to higher levels of SHM, such as the quantification of damage severity and damage prognosis.
- The MSs can be embedded in structures as contactless or inner permanent sensors (e.g., Magnetic Microwire Sensors). To resolve the power supply issue of this kind of implementation, high-performance nanogenerators and wireless power transmission techniques can be employed.
- Dynamic MSs (e.g., MR sensors) are usually designed and tested for speeds lower than 1 m/s. Developing high-speed scanning sensors is highly demanded.

CRediT authorship contribution statement

Armin Dadras Eslamlou: Writing – original draft. **Aliakbar Ghaderiaram:** Writing – original draft. **Erik Schlangen:** Writing – review & editing. **Mohammad Fotouhi:** Conceptualization, Writing – review & editing.

Declaration of Competing Interest

The authors declare that they have no known competing financial interests or personal relationships that could have appeared to influence the work reported in this paper.

Data availability

No data was used for the research described in the article.

References

[1] D. Balageas, C.-P. Fritzen, A. Güemes, Structural health monitoring, John Wiley & Sons, 2010.
[2] N. Karballaeezadeh, D. Mohammadzadeh S, S. Shamshirband, P. Hajikhodaverdikhan, A. Mosavi, K.-W. Chau, Prediction of remaining service life of pavement using an optimized support vector machine (case study of Semnan-Firuzkuh road), Eng. Appl. Comput. Fluid Mech. 13 (1) (2019) 188–198.
[3] S. W. Doebling, C. R. Farrar, M. B. Prime, and D. W. Shevitz, "Damage identification and health monitoring of structural and mechanical systems from changes in their vibration characteristics: a literature review," 1996, doi: 10.2172/249299.
[4] K. Draganová, J. Blažek, D. Praslička, F. Kmec, Possibile Applications of Magnetic Microwires in Aviation, Fatigue of Aircraft Structures 2013 (5) (2013) 12–17.
[5] P. Marín, Wireless stress sensor based on magnetic microwires, Magnetic Sensors—Development Trends and Applications (2017).
[6] L. Bottura, "Field Measurement Methods. Presentation at CERN Accelerator School (CAS) on Superconductivity," *Erice,* 2002.
[7] V.O. Jimenez, K.Y. Hwang, D. Nguyen, Y. Rahman, C. Albrecht, B. Senator, O. Thiabgoh, J. Devkota, V.D.A. Bui, D.S. Lam, T. Eggers, M.-H. Phan, Magnetoimpedance Biosensors and Real-Time Healthcare Monitors: Progress, Opportunities, and Challenges, Biosensors 12 (7) (2022) 517.
[8] A. s, On a new Action of the Magnet on Electric Currents1 Nature 21 537 1880/02/01 1880, 361 361 10.1038/021361a0.
[9] D. Zhu, X. Yi, Y. Wang, K.-M. Lee, J. Guo, A mobile sensing system for structural health monitoring: design and validation, Smart Mater. Struct. 19 (5) (2010/03/31 2010,), 055011, https://doi.org/10.1088/0964-1726/19/5/055011.
[10] B. Fernandes, D. Nims, V. Devabhaktuni, "Comprehensive MMF–MFL inspection for corrosion detection and estimation in embedded prestressing strands," *Journal of Civil*, Struct. Health Monit. 4 (1) (2014/02/01 2014,) 43–55, https://doi.org/10.1007/s13349-013-0061-4.
[11] J. Zhang, C. Liu, M. Sun, Z. Li, An innovative corrosion evaluation technique for reinforced concrete structures using magnetic sensors, Constr. Build. Mater. 135 (2017/03/15/ 2017,) 68–75, https://doi.org/10.1016/j.conbuildmat.2016.12.157.

[12] M.S. García Alonso, F. Giacomone, A. Pérez, I. Kaiser, J.F. Fernández, A. Hernando, J. Vinolas, M.A. García, Magnetostatic determination of variations of internal stress in magnetic steels, AIP Adv. 10 (11) (2020), https://doi.org/10.1063/5.0004448.

[13] W. Thomson, "XIX. On the electro-dynamic qualities of metals:—Effects of magnetization on the electric conductivity of nickel and of iron," *Proceedings of the Royal Society of London,* no. 8, pp. 546-550, 1857.

[14] A. Jander, C. Smith, R. Schneider, *Magnetoresistive sensors for nondestructive evaluation* (Nondestructive Evaluation for Health Monitoring and Diagnostics), SPIE, 2005.

[15] T. Chady, Evaluation of stress loaded steel samples using GMR magnetic field sensor, IEEE Sens. J. 2 (5) (2002) 488–493, https://doi.org/10.1109/JSEN.2002.804574.

[16] A.S.A. Kumar, B. George, S.C. Mukhopadhyay, Technologies and Applications of Angle Sensors: A Review, IEEE Sens. J. 21 (6) (2021) 7195–7206, https://doi.org/10.1109/JSEN.2020.3045461.

[17] P.I. Nicholson, M.H. So, T. Meydan, A.J. Moses, Non-destructive surface inspection system for steel and other ferromagnetic materials using magneto-resistive sensors, J. Magn. Magn. Mater. 160 (1996/07/01/ 1996,) 162–164, https://doi.org/10.1016/0304-8853(96)00156-4.

[18] B. Wincheski, J. Simpson, M. Namkung, D. Perey, E. Scales, R. Louie, Development of Giant Magnetoresistive inspection system for detection of deep fatigue cracks under airframe fasteners, AIP Conference Proceedings 615 (1) (2002) 1007–1014, https://doi.org/10.1063/1.1472906.

[19] C.C.H. Lo, J.A. Paulsen, D.C. Jiles, A magnetic imaging system for evaluation of material conditions using magnetoresistive devices, IEEE Trans. Magn. 39 (5) (2003) 3453–3455, https://doi.org/10.1109/TMAG.2003.816180.

[20] J. Popovics, G. Gallo, M. Shelton, P. Chapman, *A magnetic sensing approach to characterize corrosion in reinforced concrete* (SPIE Smart Structures and Materials + Nondestructive Evaluation and Health Monitoring), SPIE, 2007.

[21] P. Procházka, F. Vaněk, Contactless Diagnostics of Turbine Blade Vibration and Damage, J. Phys. Conf. Ser. 305 (2011/07/19 2011,), 012116, https://doi.org/10.1088/1742-6596/305/1/012116.

[22] G. Yang, G. Dib, L. Udpa, A. Tamburrino, S.S. Udpa, Rotating Field EC-GMR Sensor for Crack Detection at Fastener Site in Layered Structures, IEEE Sens. J. 15 (1) (2015) 463–470, https://doi.org/10.1109/JSEN.2014.2341653.

[23] K. Tsukada, Y. Haga, K. Morita, N. Song, K. Sakai, T. Kiwa, W. Cheng, Detection of Inner Corrosion of Steel Construction Using Magnetic Resistance Sensor and Magnetic Spectroscopy Analysis, IEEE Trans. Magn. 52 (7) (2016) 1–4.

[24] V. Zilberstein, et al., MWM eddy-current arrays for crack initiation and growth monitoring, Int. J. Fatigue 25 (9) (2003/09/01/ 2003,) 1147–1155, https://doi.org/10.1016/j.ijfatigue.2003.08.010.

[25] W. Ricken, H.C. Schoenekess, W.J. Becker, Improved multi-sensor for force measurement of pre-stressed steel cables by means of the eddy current technique, Sens. Actuators, A 129 (1) (2006/05/24/ 2006,) 80–85, https://doi.org/10.1016/j.sna.2005.11.056.

[26] H.A. Sodano, Development of an Automated Eddy Current Structural Health Monitoring Technique with an Extended Sensing Region for Corrosion Detection, Struct. Health Monit. 6 (2) (2007/06/01 2007,) 111–119, https://doi.org/10.1177/1475921706072065.

[27] D.G. Park, C.S. Angani, G.D. Kim, C.G. Kim, Y.M. Cheong, Evaluation of Pulsed Eddy Current Response and Detection of the Thickness Variation in the Stainless Steel, IEEE Trans. Magn. 45 (10) (2009) 3893–3896, https://doi.org/10.1109/TMAG.2009.2024219.

[28] Q. Cao, D. Liu, Y. He, J. Zhou, J. Codrington, Nondestructive and quantitative evaluation of wire rope based on radial basis function neural network using eddy current inspection, NDT and E Int. 46 (2012/03/01/ 2012,) 7–13, https://doi.org/10.1016/j.ndteint.2011.09.015.

[29] B. Wincheski, J. Simpson, DEVELOPMENT AND APPLICATION OF WIDE BANDWIDTH MAGNETO-RESISTIVE SENSOR BASED EDDY CURRENT PROBE, AIP Conference Proceedings 1335 (1) (2011/06/23 2011,) 388–395, https://doi.org/10.1063/1.3591879.

[30] V. Torres, S. Quek, B. Fernandes, P. Gaydecki, Development of a scanning system to detect corrosion in wire bundles and pipes using magnetoresistive sensors, Insight-Non-Destructive Testing and Condition Monitoring 53 (2) (2011) 82–84, https://doi.org/10.1784/insi.2011.53.2.82.

[31] C. Xiu, L. Ren, H. Li, Investigation on Eddy Current Sensor in Tension Measurement at a Resonant Frequency [Online]. Available: Appl. Sci. 7 (6) (2017) 538 https://www.mdpi.com/2076-3417/7/6/538.

[32] T. Chen, Y. He, J. Du, A High-Sensitivity Flexible Eddy Current Array Sensor for Crack Monitoring of Welded Structures under Varying Environment [Online]. Available: Sensors 18 (6) (2018) 1780 https://www.mdpi.com/1424-8220/18/6/1780.

[33] K. Tsukada, M. Hayashi, Y. Nakamura, K. Sakai, T. Kiwa, Small Eddy Current Testing Sensor Probe Using a Tunneling Magnetoresistance Sensor to Detect Cracks in Steel Structures, IEEE Trans. Magn. 54 (11) (2018) 1–5, https://doi.org/10.1109/TMAG.2018.2845864.

[34] M. Hayashi, T. Saito, Y. Nakamura, K. Sakai, T. Kiwa, I. Tanikura, K. Tsukada, Extraction Method of Crack Signal for Inspection of Complicated Steel Structures Using A Dual-Channel Magnetic Sensor, Sensors 19 (13) (2019) 3001.

[35] H. Sun, T. Wang, Q. Liu, Y. Wang, X. Qing, A two-dimensional eddy current array–based sensing film for estimating failure modes and tracking damage growth of bolted joints, Struct. Health Monit. 20 (3) (2021/05/01 2019,) 877–893, https://doi.org/10.1177/1475921719843062.

[36] H. Sun, T. Wang, D. Lin, Y. Wang, X. Qing, An Eddy Current-Based Structural Health Monitoring Technique for Tracking Bolt Cracking [Online]. Available: Sensors 20 (23) (2020) 6843 https://www.mdpi.com/1424-8220/20/23/6843.

[37] S. Xie, Z. Duan, J. Li, Z. Tong, M. Tian, Z. Chen, A novel magnetic force transmission eddy current array probe and its application for nondestructive testing of defects in pipeline structures, Sens. Actuators, A 309 (2020/07/01/ 2020,), 112030, https://doi.org/10.1016/j.sna.2020.112030.

[38] I. Mukherjee, J. Patil, S. Banerjee, and S. Tallur, "Phase sensitive detection of extent of corrosion in steel reinforcing bars using eddy currents," *arXiv preprint arXiv:2001.03756,* 2020.

[39] Q. Liu, H. Sun, Y. Chai, J. Zhu, T. Wang, X. Qing, On-site monitoring of bearing failure in composite bolted joints using built-in eddy current sensing film, J. Compos. Mater. 55 (14) (2021/06/01 2020,) 1893–1905, https://doi.org/10.1177/0021998320979737.

[40] R. Guilizzoni, G. Finch, S. Harmon, Subsurface Corrosion Detection in Industrial Steel Structures, IEEE Magn. Lett. 10 (2019) 1–5, https://doi.org/10.1109/LMAG.2019.2948808.

[41] J.S. Knopp, J.C. Aldrin, K.V. Jata, Computational methods in eddy current crack detection at fastener sites in multi-layer structures, Nondestructive Testing and Evaluation 24 (1–2) (2009/03/01 2009,) 103–120, https://doi.org/10.1080/10589750802195519.

[42] G. Chen, H. Mu, D. Pommerenke, J.L. Drewniak, Damage Detection of Reinforced Concrete Beams with Novel Distributed Crack/Strain Sensors, Struct. Health Monit. 3 (3) (2004/09/01 2004,) 225–243, https://doi.org/10.1177/1475921704045625.

[43] F. Rumiche, J.E. Indacochea, M.L. Wang, Assessment of the Effect of Microstructure on the Magnetic Behavior of Structural Carbon Steels Using an Electromagnetic Sensor, J. Mater. Eng. Perform. 17 (4) (2008/08/01 2008,) 586–593, https://doi.org/10.1007/s11665-007-9184-2.

[44] F. Rumiche, J.E. Indacochea, M.L. Wang, Detection and Monitoring of Corrosion in Structural Carbon Steels Using Electromagnetic Sensors, J. Eng. Mater. Technol. 130 (3) (2008) pp, https://doi.org/10.1115/1.2931145.

[45] B. Herdovics, F. Cegla, Structural health monitoring using torsional guided wave electromagnetic acoustic transducers, Struct. Health Monit. 17 (1) (2018/01/01 2016,) 24–38, https://doi.org/10.1177/1475921716682688.

[46] M. A. P. Arango, H. F. G. Mendez, and I. E. D. Pardo, "Crack Detection Using An Electromagnetic Sensor-Antenna For Structures," in *2019 Congreso Internacional de Innovación y Tendencias en Ingenieria (CONIITI)*, 2-4 Oct. 2019 2019, pp. 1-6, doi: 10.1109/CONIITI48476.2019.8960835.

[47] Z. Li, Z. Jin, X. Xu, T. Zhao, P. Wang, Z. Li, Combined application of novel electromagnetic sensors and acoustic emission apparatus to monitor corrosion process of reinforced bars in concrete, Constr. Build. Mater. 245 (2020/06/10/ 2020,), 118472, https://doi.org/10.1016/j.conbuildmat.2020.118472.

[48] Z. Li, Z. Jin, Y. Gao, T. Zhao, P. Wang, Z. Li, Coupled application of innovative electromagnetic sensors and digital image correlation technique to monitor corrosion process of reinforced bars in concrete, Cem. Concr. Compos. 113 (2020/10/01/ 2020,), 103730, https://doi.org/10.1016/j.cemconcomp.2020.103730.

[49] C. Fu, J. Huang, Z. Dong, W. Yan, X.-L. Gu, Experimental and numerical study of an electromagnetic sensor for non-destructive evaluation of steel corrosion in concrete, Sens. Actuators, A 315 (2020/11/01/ 2020,), 112371, https://doi.org/10.1016/j.sna.2020.112371.

[50] A.G. Diogenes, E.P. de Moura, A.S. Machado, L.L. Gonçalves, Determination of Carbon Steel Bar Diameter by Nondestructive Magnetic Testing, J. Nondestr. Eval. 40 (3) (2021/06/25 2021,) 59, https://doi.org/10.1007/s10921-021-00791-9.

[51] P.K. Frankowski, T. Chady, A. Zieliński, Magnetic force induced vibration evaluation (M5) method for frequency analysis of rebar-debonding in reinforced concrete, Measurement 182 (2021/09/01/ 2021,), 109655, https://doi.org/10.1016/j.measurement.2021.109655.

[52] S. Sumitro, S. Kurokawa, K. Shimano, M.L. Wang, Monitoring based maintenance utilizing actual stress sensory technology, Smart Mater. Struct. 14 (3) (2005/05/26 2005,) S68–S78, https://doi.org/10.1088/0964-1726/14/3/009.

[53] G. Ausanio, A.C. Barone, C. Hison, V. Iannotti, G. Mannara, L. Lanotte, Magnetoelastic sensor application in civil buildings monitoring, Sens. Actuators, A vol. 123–124 (2005/09/23/ 2005,) 290–295, https://doi.org/10.1016/j.sna.2005.03.027.

[54] J. Kim, J.-W. Kim, C. Lee, S. Park, Development of Embedded EM Sensors for Estimating Tensile Forces of PSC Girder Bridges, Sensors 17 (9) (2017) pp, https://doi.org/10.3390/s17091989.

[55] L. Ren, C. Xiu, H. Li, Y. Lu, J. Wang, X. Yao, Development of elasto-magnetic (EM) sensor for monitoring cable tension using an innovative ratio measurement method, Smart Mater. Struct. 27 (11) (2018/09/25 2018,), 115003, https://doi.org/10.1088/1361-665x/aae0b0.

[56] R. Zhang, Y. Duan, Y. Zhao, X. He, Temperature Compensation of Elasto-Magneto-Electric (EME) Sensors in Cable Force Monitoring Using BP Neural Network, Sensors 18 (7) (2018) pp, https://doi.org/10.3390/s18072176.

[57] S. Zhang, J. Zhou, Y. Zhou, H. Zhang, J. Chen, Cable Tension Monitoring Based on the Elasto-Magnetic Effect and the Self-Induction Phenomenon, Materials 12 (14) (2019) pp, https://doi.org/10.3390/ma12142230.

[58] J. Kim, S. Park, Field applicability of a machine learning–based tensile force estimation for pre-stressed concrete bridges using an embedded elasto-magnetic sensor, Struct. Health Monit. 19 (1) (2020/01/01 2019,) 281–292, https://doi.org/10.1177/1475921719842340.

[59] J. Kim, J.-W. Kim, S. Park, Investigation of Applicability of an Embedded EM Sensor to Measure the Tension of a PSC Girder, Journal of Sensors 2019 (2019/03/31 2019,) 2469647, https://doi.org/10.1155/2019/2469647.

[60] H. Feng, X. Liu, B. Wu, D. Wu, X. Zhang, C. He, Temperature-insensitive cable tension monitoring during the construction of a cable-stayed bridge with a custom-developed pulse elasto-magnetic instrument, Struct. Health Monit. 18 (5–6) (2019/11/01 2018,) 1982–1994, https://doi.org/10.1177/1475921718814733.

[61] S. Zhang, J. Zhou, H. Zhang, L. Liao, L. Liu, Influence of cable tension history on the monitoring of cable tension using magnetoelastic inductance method, Struct. Health Monit. 20 (6) (2021/11/01 2021,) 3392–3405, https://doi.org/10.1177/1475921720987987.

[62] S. Park J.-W. Kim C. Lee J.-J. Lee Magnetic Flux Leakage Sensing-Based Steel Cable NDE Technique Shock and Vibration 2014 2014 1 8 929341.

[63] Y. Sun, S. Liu, R. Li, Z. Ye, Y. Kang, S. Chen, A new magnetic flux leakage sensor based on open magnetizing method and its on-line automated structural health monitoring methodology, Struct. Health Monit. 14 (6) (2015) 583–603, https://doi.org/10.1177/1475921715604387.

[64] K. Sakai, K. Morita, Y. Haga, T. Kiwa, K. Inoue, K. Tsukada, Automatic Scanning System for Back-Side Defect of Steel Structure Using Magnetic Flux Leakage Method, IEEE Trans. Magn. 51 (11) (2015) 1–3, https://doi.org/10.1109/TMAG.2015.2453211.

[65] S. Park, J.-W. Kim, D.-J. Moon, *Non-contact main cable NDE technique for suspension bridge using magnetic flux-based B-H loop measurements* (SPIE Smart Structures and Materials + Nondestructive Evaluation and Health Monitoring), SPIE, 2015.

[66] J.-W. Kim, J. Kim, S. Park, Cross-Sectional Loss Quantification for Main Cable NDE Based on the B-H Loop Measurement Using a Total Flux Sensor, Journal of Sensors 2019 (2019/10/09 2019,) 8014102, https://doi.org/10.1155/2019/8014102.

[67] J.-W. Kim, S. Park, Magnetic flux leakage–based local damage detection and quantification for steel wire rope non-destructive evaluation, J. Intell. Mater. Syst. Struct. 29 (17) (2018) 3396–3410, https://doi.org/10.1177/1045389x17721038.

[68] J.-W. Kim S. Park Magnetic Flux Leakage Sensing and Artificial Neural Network Pattern Recognition-Based Automated Damage Detection and Quantification for Wire Rope Non-Destructive Evaluation Sensors 18 1 109.

[69] H. Zhang L. Liao R. Zhao J. Zhou M. Yang R. Xia The Non-Destructive Test of Steel Corrosion in Reinforced Concrete Bridges Using a Micro-Magnetic Sensor Sensors 16 9 1439.

[70] R. Xia, J. Zhou, H. Zhang, D. Zhou, Z. Zhang, Experimental Study on Corrosion of Unstressed Steel Strand based on Metal Magnetic Memory, KSCE J. Civ. Eng. 23 (3) (2019/03/01 2019,) 1320–1329, https://doi.org/10.1007/s12205-019-0715-9.

[71] M. Mosharafi, S.B. Mahbaz, M.B. Dusseault, P. Vanheeghe, Magnetic detection of corroded steel rebar: Reality and simulations, NDT and E Int. 110 (2020/03/01/2020,), 102225, https://doi.org/10.1016/j.ndteint.2020.102225.

[72] Y. Sun, S. Liu, Z. Deng, R. Tang, W. Ma, X. Tian, Y. Kang, L. He, Magnetic flux leakage structural health monitoring of concrete rebar using an open electromagnetic excitation technique, Struct. Health Monit. 17 (2) (2018) 121–134.

[73] Zhang Jing Xu Zhan Tan A Sensor for Broken Wire Detection of Steel Wire Ropes Based on the Magnetic Concentrating Principle Sensors 19 17 3763.

[74] A. Elyasigorji, M. Rezaee, A. Ghorbanpoor, Magnetic Corrosion Detection in Concrete Structures, International Conference on Sustainable Infrastructure 2019 (2019) 175–184.

[75] A. Elyasigorji, M. Rezaee, A. Ghorbanpoor, Characterization of Corrosion in PS Concrete Girders by Correlation Analysis, Structures Congress 2020 (2020) 285–292.

[76] A. Ghorbanpoor, R. Borchelt, M. Edwards, and E. A. Salam, "Magnetic-Based NDE of Prestressed and Post-Tensioned Concrete Members: The MFL System," (in English), Research Paper 2000. [Online]. Available: https://rosap.ntl.bts.gov/view/dot/15359.

[77] H. Azari, A. Ghorbanpoor, S. Shams, Development of Robotic Nondestructive Testing of Steel Corrosion of Prestressed Concrete Bridge Girders using Magnetic Flux Leakage System, Transp. Res. Rec. 2674 (8) (2020) 466–476, https://doi.org/10.1177/0361198120925471.

[78] M. Hayashi, T. Kawakami, T. Saito, K. Sakai, T. Kiwa, K. Tsukada, Imaging of Defect Signal of Reinforcing Steel Bar at High Lift-Off Using a Magnetic Sensor Array by Unsaturated AC Magnetic Flux Leakage Testing, IEEE Trans. Magn. 57 (2) (2021) 1–4, https://doi.org/10.1109/TMAG.2020.3017722.

[79] L.E. Mujica, M. Ruiz, R. Villamizar, Multidimensional data statistical processing of magnetic flow leakage signals from a Colombian gas pipeline, Struct. Health Monit. 20 (6) (2021) 2963–2992, https://doi.org/10.1177/1475921720977393.

[80] A. Zagrai, H. Cakan, Magneto-mechanical impedance technique for dynamic identification of metallic structures, in: In *Proc. of 6th International Workshop on Structural Health MonitorIng*, 2007, pp. 11–13.

[81] A. Zagrai, H. Çakan, *Damage diagnostics of metallic structures using magneto-mechanical impedance technique* (SPIE Smart Structures and Materials + Nondestructive Evaluation and Health Monitoring), SPIE, 2008.

[82] D. Doyle, A. Zagrai, B. Arritt, H. Çakan, Damage Detection in Bolted Space Structures, J. Intell. Mater. Syst. Struct. 21 (3) (2010/02/01 2009,) 251–264, https://doi.org/10.1177/1045389X09354785.

[83] A.N. Zagrai, H. Çakan, Magneto-mechanical impedance identification and diagnosis of metallic structures, Int. J. Eng. Sci. 48 (10) (2010/10/01/ 2010,) 888–908, https://doi.org/10.1016/j.ijengsci.2010.05.010.

[84] Q. Shuai, J. Tang, Enhanced modeling of magnetic impedance sensing system for damage detection, Smart Mater. Struct. 23 (2) (2013/12/23 2013,), 025008, https://doi.org/10.1088/0964-1726/23/2/025008.

[85] Q. Shuai, J. Tang, *Improved modeling of magnetic impedance sensing system for damage detection* (SPIE Smart Structures and Materials + Nondestructive Evaluation and Health Monitoring), SPIE, 2013.

[86] M. Roskosz, K. Fryczowski, Magnetic methods of characterization of active stresses in steel elements, J. Magn. Magn. Mater. 499 (2020/04/01/ 2020,), 166272, https://doi.org/10.1016/j.jmmm.2019.166272.

[87] P. Szulim S. Gontarz Extraction of Magnetic Field Features to Determine the Degree of Material Strain Materials 14 6 1576.

[88] A. Al-Hajjeh, E. Lynch, C.T. Law, R. El-Hajjar, Characteristics of a Magnetostrictive Composite Stress Sensor, IEEE Magn. Lett. 7 (2016) 1–4, https://doi.org/10.1109/LMAG.2016.2540613.

[89] Z. Fang, P.W. Tse, Axial magnetized patch for efficient transduction of longitudinal guided wave and defect identification in concrete-covered pipe risers, Struct. Control Health Monit. 25 (10) (2018) e2231.

[90] Z. Fang, P.W. Tse, Demagnetization-based axial magnetized magnetostrictive patch transducers for locating defect in small-diameter pipes using the non-axisymmetric guided wave, Struct. Health Monit. 18 (5–6) (2019/11/01 2019,) 1738–1760, https://doi.org/10.1177/1475921719833471.

[91] A. Gullapalli, V. Beedasy, J.D.S. Vincent, Z. Leong, P. Smith, N. Morley, Flat Inkjet-Printed Copper Induction Coils for Magnetostrictive Structural Health Monitoring: A Comparison with Bulk Air Coils and an anisotropic magnetoresistive sensor (AMR) Sensor, Adv. Eng. Mater. 23 (9) (2021) 2100313, https://doi.org/10.1002/adem.202100313.

[92] J. Olivera, M. Gonzalez, J.V. Fuente, R. Varga, A. Zhukov, J.J. Anaya, An embedded stress sensor for concrete SHM based on amorphous ferromagnetic microwires, Sensors (Basel) 14 (11) (2014) 19963–19978, https://doi.org/10.3390/s141119963.

[93] S. Atalay, V.S. Kolat, N. Bayri, T. Izgi, Magnetoelastic Sensor Studies on Amorphous Magnetic FeSiB Wire and the Application in Viscosity Measurement, J. Supercond. Nov. Magn. 29 (6) (2016) 1551–1556, https://doi.org/10.1007/s10948-016-3440-3.

[94] M. Churyukanova, S. Kaloshkin, E. Shuvaeva, A. Stepashkin, M. Zhdanova, A. Aronin, O. Aksenov, P. Arakelov, V. Zhukova, A. Zhukov, Non-contact method for stress monitoring based on stress dependence of magnetic properties of Fe-based microwires, J. Alloy. Compd. 748 (2018) 199–205.

[95] Olivera Aparicio Hernández Zhukov Varga Campusano Echavarria Velayos Microwire-Based Sensor Array for Measuring Wheel Loads of Vehicles Sensors 19 21 4658.

[96] M. Al Ali, P. Platko, V. Bajzecerova, S. Kmet, L. Galdun, A. Spegarova, R. Varga, Monitoring the strain of beech plywood using a bistable magnetic microwire, Sens. Actuators, A 326 (2021) 112726.

[97] M.A. Ali S. Kmeť P. Platko V. Bajzecerová M. Zeleňáková The Design and Production of a Suitable Carrier for Microwires Used for Non-Contact Detection of Mechanical Strains Sustainability 13 2 477.

[98] G. Chen, B.P. Schafer, Z. Lin, Y. Huang, O. Suaznabar, J. Shen, K. Kerenyi, Maximum scour depth based on magnetic field change in smart rocks for foundation stability evaluation of bridges, Struct. Health Monit. 14 (1) (2015) 86–99.

[99] F. Tang, Y. Chen, Z. Li, X. Hu, G. Chen, Y. Tang, Characterization and field validation of smart rocks for bridge scour monitoring, Struct. Health Monit. 18 (5–6) (2019/11/01 2019,) 1669–1685, https://doi.org/10.1177/1475921718824944.

[100] H. Zhang, Z. Li, G. Chen, A. Reven, B. Scharfenberg, J. Ou, "UAV-based smart rock localization for bridge scour monitoring," *Journal of Civil*, Struct. Health Monit. 11 (2) (2021/04/01 2021,) 301–313, https://doi.org/10.1007/s13349-020-00453-w.

[101] Z. Zhixiang, Z. Benniu, X. Kaiwen, L. Xingxing, Y. Guo, Z. Kaihong, Smart film for crack monitoring of concrete bridges, Struct. Health Monit. 10 (3) (2011/05/01 2010,) 275–289, https://doi.org/10.1177/1475921710373288.

[102] J.H. Kurz, L. Laguerre, F. Niese, L. Gaillet, K. Szielasko, R. Tschuncky, F. Treyssede, "NDT for need based maintenance of bridge cables, ropes and pre-stressed elements," *Journal of Civil*, Struct. Health Monit. 3 (4) (2013) 285–295.

[103] O. Kypris, A. Markham, 3-D Displacement Measurement for Structural Health Monitoring Using Low-Frequency Magnetic Fields, IEEE Sens. J. 17 (4) (2017) 1165–1174, https://doi.org/10.1109/JSEN.2016.2636451.

[104] A. Davis, M. Mirsayar, E. Sheahan, D. Hartl, *Structural health monitoring for DOT using magnetic shape memory alloy cables in concrete* (SPIE Smart Structures and Materials + Nondestructive Evaluation and Health Monitoring), SPIE, 2018.

[105] K. Pospisil M. Manychova J. Stryk M. Korenska R. Matula V. Svoboda Diagnostics of Reinforcement Conditions in Concrete Structures by GPR, Impact-Echo Method and Metal Magnetic Memory Method Remote Sensing 13 5 952.

[106] S. Yin, D. Song, X. He, L. Qiu, Z. Li, Q. Lou, J. Li, Y. Liu, Experimental study on the change of magnetic field in the process of concrete failure under load, Struct. Control Health Monit. 28 (10) (2021) e2806, https://doi.org/10.1002/stc.2806.

[107] A.M. Nazar, P. Jiao, Q. Zhang, K.J.I. Egbe, A.H. Alavi, A New Structural Health Monitoring Approach Based on Smartphone Measurements of Magnetic Field Intensity, IEEE Instrum. Meas. Mag. 24 (4) (2021) 49–58, https://doi.org/10.1109/MIM.2021.9448251.

[108] S. Almahmoud O. Shiryayev N. Vahdati P. Rostron Detection of Internal Metal Loss in Steel Pipes and Storage Tanks via Magnetic-Based Fiber Optic Sensor Sensors 18 3 815.

[109] S. Almahmoud, O. Shiryayev, N. Vahdati, P. Rostron, *Pipeline internal corrosion sensor based on fiber optics and permanent magnets* (SPIE Smart Structures and Materials + Nondestructive Evaluation and Health Monitoring), SPIE, 2018.
[110] O. Shiryayev, M. Cullin, R. Srinivasan, *On the development of an improved magnetic-based corrosion sensor* (SPIE Smart Structures + Nondestructive Evaluation), SPIE, 2021.
[111] I. Lei, X. Jin, Y.e. Tian, X. Lin, N. Jin, D. Yan, Z. Li, W. Zheng, X. Sun, H. Lin, Y. Yan, Z. Xu, "Numerical simulation of a magnetic corrosion detector for corrosion detection of steel rebar in concrete," *Journal of Civil*, Struct. Health Monit. 12 (1) (2022) 1–14.
[112] M. M. Andringa, D. P. Neikirk, N. P. Dickerson, and S. L. Wood, "Unpowered wireless corrosion sensor for steel reinforced concrete," in *SENSORS, 2005 IEEE*, 30 Oct.-3 Nov. 2005 2005, p. 4 pp., doi: 10.1109/ICSENS.2005.1597659.
[113] J.-M. Kim, M. Han, H. Sohn, Magnetic resonance-based wireless power transmission through concrete structures, Journal of electromagnetic engineering and science 15 (2) (2015) 104–110, https://doi.org/10.5515/JKIEES.2015.15.2.104.
[114] J. Lu, M. Gao, Y. Wang, P. Wang, Health monitoring of urban rail corrugation by wireless rechargeable sensor nodes, Struct. Health Monit. 18 (3) (2019/05/01 2018,) 838–852, https://doi.org/10.1177/1475921718782395.
[115] A. Hosseinkhani, D. Younesian, P. Eghbali, A. Moayedizadeh, A. Fassih, Sound and vibration energy harvesting for railway applications: A review on linear and nonlinear techniques, Energy Rep. 7 (2021/11/01/ 2021,) 852–874, https://doi.org/10.1016/j.egyr.2021.01.087.
[116] M. Gao, P. Wang, Y. Cao, R. Chen, D. Cai, Design and Verification of a Rail-Borne Energy Harvester for Powering Wireless Sensor Networks in the Railway Industry, IEEE Trans. Intell. Transp. Syst. 18 (6) (2017) 1596–1609, https://doi.org/10.1109/TITS.2016.2611647.
[117] Z. Wang A. Markham Wirelessly Powered Embedded Sensor Nodes for Internal Structural Health Monitoring IEEE Transactions on Industrial Electronics 2020 1 1 10.1109/TIE.2020.3013536.
[118] M.O. Furkan, Q. Mao, S. Livadiotis, M. Mazzotti, A.E. Aktan, S.P. Sumitro, I. Bartoli, "Towards rapid and robust measurements of highway structures deformation using a wireless sensing system derived from wired sensors," *Journal of Civil*, Struct. Health Monit. 10 (2) (2020) 297–311.
[119] I. Altpeter, G. Dobmann, M. Kröning, M. Rabung, S. Szielasko, Micro-magnetic evaluation of micro residual stresses of the IInd and IIIrd order, NDT and E Int. 42 (4) (2009/06/01/ 2009,) 283–290, https://doi.org/10.1016/j.ndteint.2008.11.007.